ORNL/TM-2018/901

External Cooling of the BWR Mark I and II Drywell Head as a Potential Accident Mitigation Measure: Expanded Scoping Assessment

Kevin R. Robb

July 2018

OAK RIDGE NATIONAL LABORATORY
MANAGED BY UT-BATTELLE FOR THE US DEPARTMENT OF ENERGY

ORNL/TM-2018/901

Reactor Safety Technologies – Light Water Reactor Sustainability Program

External Cooling of the BWR Mark I and II Drywell Head as a Potential Accident Mitigation Measure: Expanded Scoping Assessment

Kevin R. Robb

Date Published:
July 2018

Work Package#: LW-18OR100603
Milestone #: M3LW-18OR1006033

Prepared by
OAK RIDGE NATIONAL LABORATORY
Oak Ridge, Tennessee 37831-6283
managed by
UT-BATTELLE, LLC
for the
US DEPARTMENT OF ENERGY
under contract DE-AC05-00OR22725

CONTENTS

Page

LIST OF FIGURES

Figure **Page**

LIST OF TABLES

Table **Page**

ACRONYMS AND ABBREVIATIONS

AC	alternating current
BWR	boiling water reactor
CFR	US Code of Federal Regulations
CV	control volume
DC	direct current
DW	drywell
ELAP	extended loss of AC power
FLEX	Diverse and Flexible Coping Strategies
HPCI	high pressure coolant injection system
LTSBO	long-term station blackout
NRC	US Nuclear Regulatory Commission
ORNL	Oak Ridge National Laboratory
PCV	primary containment vessel
RCIC	reactor core isolation cooling system
RCP	reactor coolant pump
RPV	reactor pressure vessel
SOARCA	State of the Art Reactor Consequence Analysis
SBO	station blackout
SRV	safety relief valve
T&P	temperature and pressure

ACKNOWLEDGMENTS

This work was supported through the Light Water Reactor Sustainability Reactor Safety Technologies pathway within the US Department of Energy Office of Nuclear Energy. The author would like to recognize the thoughtful reviews by Scott Greenwood and Robert Salko at Oak Ridge National Laboratory.

ABSTRACT

This report documents a scoping assessment of a potential accident mitigation action applicable to the US fleet of boiling water reactors with Mark I and II containments. The mitigation action is to externally flood the primary containment vessel drywell head using portable pumps or other means. A scoping assessment of the potential benefits of this mitigation action was conducted focusing on the ability to (1) passively remove heat from containment, (2) prevent or delay leakage through the drywell head seal (due to high temperatures and/or pressure), and (3) scrub radionuclide releases if the drywell head seal leaks. This report is an expanded revision of ORNL/TM-2017/457 and includes an analysis of (1) the delay in initiating drywell head cavity flooding from 2 hours to 8 hours after accident scenario initiation and (2) the effectiveness of including additional drywell head heat transfer area.

1. INTRODUCTION AND BACKGROUND

1.1 STUDY OBJECTIVES AND FOCUS

This study is a scoping assessment of a potential accident mitigation action applicable to boiling water reactors (BWRs) with Mark I and II containments. The action is to externally flood the primary containment vessel (PCV) drywell (DW) head using portable pumps or other means. The potential benefits of this mitigation action are assessed focusing on its ability to:

1. passively remove heat from containment to reduce pressurization and extend coping time,
2. prevent or delay failure of the DW head due to high temperatures and/or pressure, and
3. scrub radionuclide releases if the DW head seal does leak.

This report is an expanded revision of ORNL/TM-2017/457 [1]. In the previous analysis, the DW head cavity flooding was initiated two hours after the accident scenario was initiated. This report investigates the impact of delaying the initiation of flooding to eight hours after the start of the accident scenarios. This report also investigates the impact of including additional DW head heat transfer surface area on the effectiveness of mitigation measure. The content of ORNL/TM-2017/457 is retained in this report for the ease of the reader.

Background information relevant to this potential mitigation action is provided in Section 1. The potential heat transfer, water injection requirements, head loading, and scrubbing efficacy are discussed and analytically investigated in Section 2. Integral analysis of the mitigation action for simulated station blackout (SBO) accident scenarios are discussed in Section 4. The model setup for the integral analyses is discussed in Section 3. Finally, conclusions and recommendations are provided in Section 5.

1.2 STUDY LIMITATIONS

It is stressed that this is a scoping assessment of the potential effects resulting from the proposed mitigation action. Only select considerations and two prescribed accident scenarios were investigated. Many other considerations are not discussed, including cost-benefit analyses, plant-specific differences from that assumed in this analysis, other accident scenarios, human factors, seismic considerations, the potential impact on other accident mitigation actions, etc. This study is viewed as a first step in the assessment of such an accident mitigation action.

1.3 SYSTEM DESCRIPTION

The BWR Mark I and II containments are illustrated in Figure 1.The PCVs are steel-lined structures located inside a secondary containment/reactor building. The containments are subdivided into two parts; the wetwell and the DW. The wetwell contains a large volume of water used to condense steam during an accident, thereby limiting containment pressurization. The wetwell can also scrub radionuclide releases from the reactor pressure vessel (RPV). The DW encompasses the RPV and other supporting equipment. The removable DW head is at the top of the DW. The DW head has an ellipsoid shape and is bolted to the DW liner. The flange design varies between units, with differences in the number and length of the bolts. The DW head resides in a reinforced concrete cavity. Two to three layers of large, reinforced, segmented concrete shield plugs are across the top of the cavity. Clearance gaps between and around the shield plugs facilitate their practical placement. The refueling bay is above the shield plugs and is where the spent fuel pool is accessed. During refueling, the shield plugs, DW head, and top of the RPV are removed, and the cavity is flooded with water. Gates connecting the spent fuel pool to the DW head cavity are opened to enable movement of fuel assemblies between the RPV and spent fuel pool.

As noted by Shah et al. [2], there is a two- to three-inch (5–7.5 cm) gap between the DW liner and the concrete shield wall in the upper portions of the PCV in Mark I and II containments. Based on a survey of 24 earlier builds, a compressible material that is generally made of foam or fiberglass was placed in this gap during construction. Shah et al. note that this material was removed in some plants, while it remained in place at others. For the current study, water ingression into the gap was not considered.

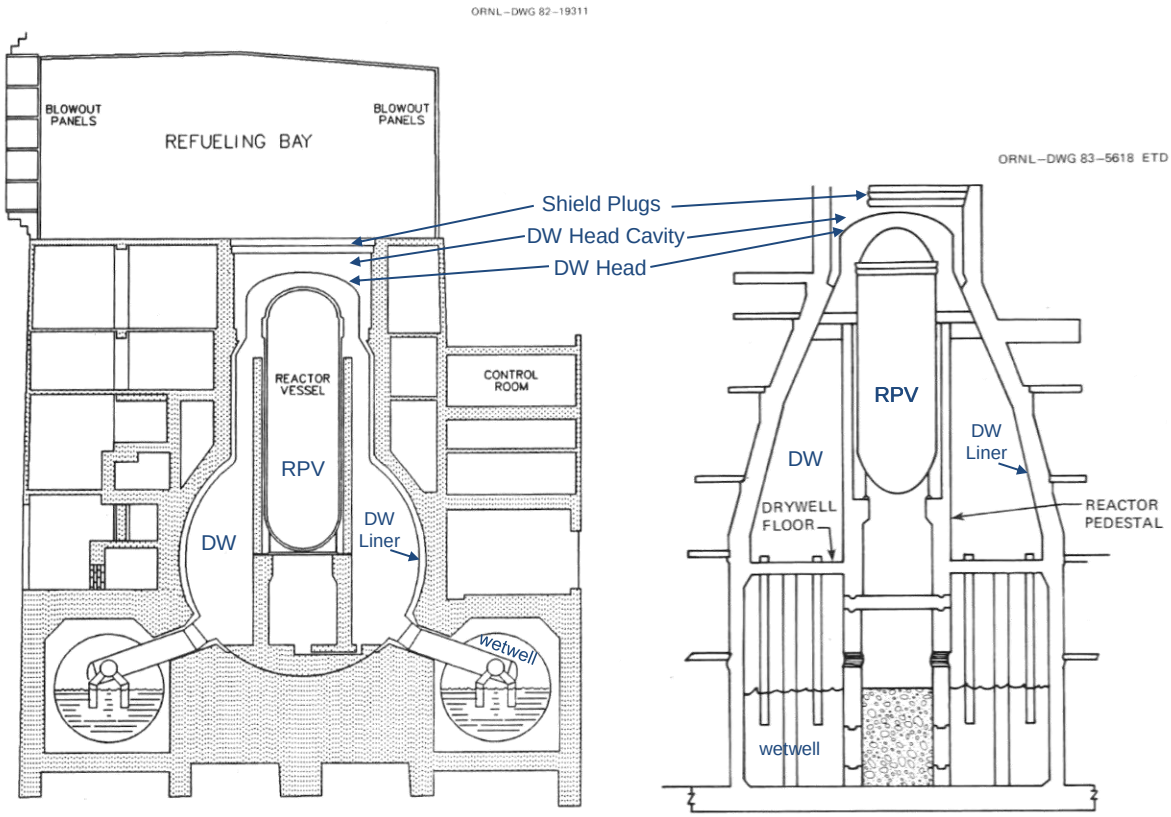

Figure 1. Example BWR Mark-1 (left) and Mark-2 (right) containments [3] with labels.

1.4 MARK I CONTAINMENT PERFORMANCE DURING EVENTS AT FUKUSHIMA DAIICHI

Three BWRs with Mark I containments at Fukushima Daiichi in Japan experienced extended station blackouts that initiated on March 11, 2011 [3]. Description, review, and assessment of the events at Fukushima Daiichi are discussed in detail in the literature. The following section briefly reviews the data, observations, and simulation efforts related to DW pressure and the DW head's potential to leak during an extended station blackout.

1.4.1 Accident Data and Observations

Available data [5] for DW pressure of units 1F1, 1F2, and 1F3 are provided in Figure 2. These data span five days after the event initiation. As observed, DW pressure was elevated and varied for extended periods of time for all three units. Both 1F1 and 1F2 DWs had sustained pressures greater than 0.7 MPa for approximately 10 hours.

Combustion events in the reactor building, or *secondary containment*, occurred at 1F1 and 1F3 [3]. Leakage through the DW head flange seal is a possible path for hydrogen to migrate from the PCV to the reactor building.

Post-event observations in 2016 and 2017 of 1F1 shield plugs indicate that they had been displaced, and dose surveys indicated elevated doses above the shield plugs at all three units [6,7,8]. Thermal images of 1F1, taken in October 2011, indicate elevated temperatures above the shield plugs that are located above the DW head [9].

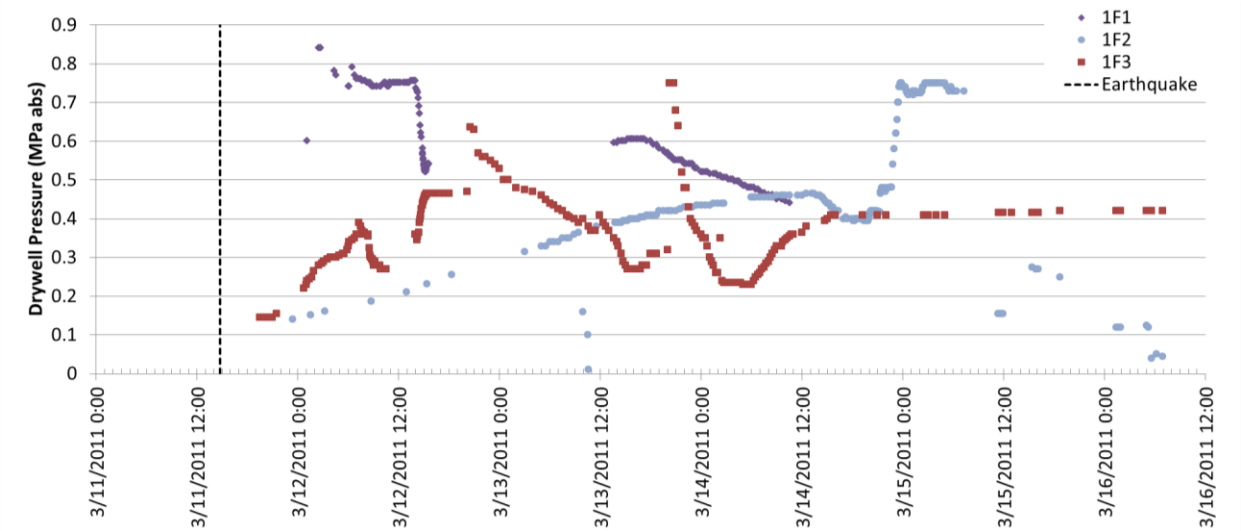

Figure 2. DW pressure data from Fukushima Daiichi Units 1–3.

1.4.2 Code Predictions

Following the events at Fukushima Daiichi, simulations were conducted for the three units using the MELCOR [10] and MAAP [12,13] codes. MELCOR simulations of 1F1 predicted that DW head leakage through the flange seal due to high DW pressures during the accident [10]. Simulations modeled the DW head leakage area as a function of containment pressure. This model is discussed in further detail in Section 3.3.4.2. Analysis using the MAAP code also attributed the DW pressure response for 1F1, 1F2 and 1F3 to DW head flange seal leakage [10,13]. For 1F1, MELCOR and MAAP simulations predict a flow area on the order of 4.5–7.5 cm^2 during leakage through the DW head flange seal [10,11,12]. In general, leakage through the DW head flange seal allowed for hydrogen (and potentially carbon monoxide) to enter the refueling bay and led to the combustion events in 1F1 and 1F3. Also, radionuclides released through this path can bypass the scrubbing capability of the wetwell and contributed to the offsite releases.

1.5 ACCIDENT MITIGATION CAPABILITIES

Nuclear power plants can respond to accidents within and beyond their design bases. Recently, additional enhancements to plants' coping capabilities have been made related to the proposed mitigation action.

Following the September 11, 2001 terrorist attacks, the US Nuclear Regulatory Commission (NRC) imposed the Interim Compensatory Measures (Order EA-02-026) and later codified the measures in the US Code of Federal Regulations (CFR). As noted in 10 CFR 50.54(hh)(2):

Each licensee shall develop and implement guidance and strategies intended to maintain or restore core cooling, containment, and spent fuel pool cooling capabilities under the circumstances associated with loss of large areas of the plant due to explosions or fire, to include strategies in the following areas: (i) Fire fighting; (ii) Operations to mitigate fuel damage; and (iii) Actions to minimize radiological release.

The enhancements the plants made to satisfy these requirements are generally termed the *B.5.b capabilities*, referring to a section of Order EA-02-026, Attachment 2 that remains official use only.

In response to the 2011 events at the Fukushima Daiichi plant, the industry developed and implemented Diverse and Flexible Coping Strategies (FLEX) [14], which includes equipment, staging, procedures and guidelines, and programmatic controls to increase plants' defense-in-depth ability to response to external events beyond design basis. Onsite and off-site equipment that can be brought onsite includes portable pumps, generators, batteries, hoses, tools, etc.

Pre-existing onsite capabilities, additional portable pumps and equipment as part of FLEX, and potentially the B.5.b capabilities can be used to provide water to the DW head cavity during an event.

1.6 POTENTIAL MITIGATION ACTION AND EFFECTS

During accident scenarios such as a station blackout or extended loss of AC power, the reactor is successfully shut down, but decay heat continues to be generated. Before core damage, this heat results in steam. The steam is generally vented to the wetwell where it condenses. If the wetwell cannot be cooled, the wetwell temperature and containment pressure will gradually increase. Eventually, without cooling, the wetwell will become saturated and be unable to condense steam. After this point, the containment temperature and pressure will increase faster. If the temperature and/or pressure of the containment exceed component stress/strain limits, the containment may leak and release radionuclides to the environment.

The proposed mitigation action is to externally inject water through the shield plugs into the DW head cavity above the PCV. The mitigation action is applicable to accident scenarios where there is an extended loss of core cooling and/or containment cooling. The water could be introduced through the clearance gaps around the periphery and between shield plug segments. This water would impact and remove heat from the DW head. The heat transfer would augment condensation in the DW, lowering containment pressure and temperature. The slower containment pressurization may extend the plant's coping time with respect to manual containment venting or containment failure. Also, the water in the cavity may aid in scrubbing radionuclides if the DW head seal were to eventually leak.

2. PARAMETRIC SCOPING STUDIES

2.1 ASSUMED GEOMETRY

Table 1 and Table 2 summarize the assumed geometry of the PCV liner and head, as well as the concrete cavity in the region of interest. For the purposes of the scoping study, the assumed geometry is deemed representative of the Mark–I DW head region. However, actual plant dimensions may vary.

The DW head is assumed to be ellipsoid in shape with a radius of 4.9 m and height of 2.45 m. Between the ellipsoid head and the flange, there is a cylindrical section with a radius of 4.9 m and a height of 1.2m. Another cylindrical section between the flange and the liner-to-shield wall seal is assumed to be 4.9 m in radius and 1.0 m in height. The head and liner thickness in this region is assumed to be 0.0381 m (1.5 in.) thick.

The assumed geometry of the DW head cavity is a cylinder with a radius of 6.1 m (20 ft), and 5.4 m (17.75 ft) of free height. The concrete shield plugs are assumed to have a combined total thickness of 1.8 m.

Additional structures that may be present in the cavity are not modeled or otherwise accounted for.

Table 1. Summary of geometry

DW head segment	Radius (m)	Segment height (m)	Gas volume inside (m^3)	Structure mass (kg)	Inside surface area (m^2)	Outside surface area (m^2)
Elliptic head	4.9	2.45	119.4	29,420	102.9	104.2
Upper cylindrical section	4.9	1.2	89.1	10,870	36.7	36.9
Low cylindrical section	4.9	1.0	74.3	9,060	30.5	30.8
Total	NA	NA	282.8	49,350	170.1	171.9

Table 2. Volumes vs. elevation

Relative Elevation (m)	Cumulative gas volume (m^3)		Notes
	Internal	External	
0	0.00	0.00	Bottom of cavity
0.5	37.13	20.73	
1.0	74.26	41.47	DW head flange seal face
1.6	118.82	66.35	
2.2	163.37	91.23	Cylinder-elliptical head transition
2.7	199.97	112.49	
3.2	233.38	136.89	
3.6	255.66	160.78	
4.0	272.23	190.31	
4.4	281.44	227.07	
4.65	282.74	254.43	Top of DW head
5.0	282.74	295.35	
5.4	282.74	344.44	Bottom of shield plugs

2.2 HEAT TRANSFER ANALYSIS

The following section provides a scoping assessment of the potential heat removal from the DW via heat transfer through the DW head and nearby liner to water in the DW head cavity. The influence of (1) containment pressure and (2) the presence of noncondensable gases inside the DW on the heat removal are considered.

The accident mitigation measure is to inject water through the concrete shield plugs above the DW. The subcooled water would impact the DW head. Depending on the temperature of the head, the water would either boil or convectively remove heat. Vapor could pass through the gaps in the shield plugs. Depending on the heat transfer and water injection rate, water would either boil off or accumulate in the cavity.

This section uses the following assumptions:

- The containment is modeled as one large volume and does not consider the complexities of the wetwell (e.g., impact on humidity/steam, compartmentalization of noncondensables)
- The steam/nitrogen mixture in the DW is well mixed. There is no stratification other than the usual gradient that will occur at the condensation interface
- Any hydrogen in containment stratifies at the top of the DW
- No heat transfer occurs through the stratified volume of hydrogen.
- All gases act as ideal gases
- The condensation heat transfer coefficient is constant for all DW head surface orientations (this approximation is within ~15–25% [15])
- The bulk flow of steam in the DW to the head region is sufficient to offset the steam condensation rate (i.e., this is not the rate limiting process)

The assumed values for various key parameters are defined in Table 3.

Table 3. Key parameters for heat transfer calculations

Parameter	Value
Thermal conductivity of DW carbon steel liner, k_{steel} (W/m-K) (MELCOR default for carbon steel at 100°C [16])	44.23
Thickness of DW liner, δ (cm)	3.81
Volume of the DW, $V_{containment}$ (m^3)	4,275
DW initial pressure (Pa)	101,325
DW initial temperature (°C)	63
DW initial relative humidity	0.20
Convective heat transfer coefficient on liner/head outer surface, $h_{convection}$, (W/m K)	30
Water temperature if boiling is not occurring, T_{pool}, (°C)	40

2.2.1 DW Gas Mass and Pressure Relationships

The masses and concentrations of steam, nitrogen, and hydrogen in the DW will vary over the course of an accident. The Mark I and II containments are initially back-filled with nitrogen. Water vapor can be introduced through normal leakage of the primary system, failures of the primary system such as main steam line creep rupture, gaseous flow from the pressure suppression pool, etc. Hydrogen resulting from oxidation of cladding and other materials can also be introduced into the DW. There is the possibility for CO, CO_2, and SiO_2 to be introduced into containment through core-concrete interactions, but these gases

are not addressed here. The pressure and concentration of the gases can affect the heat transfer through the DW head.

2.2.1.1 Treatment of hydrogen

During an accident, hydrogen can be produced via steam oxidation of zirconium-based fuel rods and channel boxes, B_4C control material, and stainless steel structures. Hydrogen is significantly less dense than steam or nitrogen. Due to the differences in density and the condensation of steam, hydrogen may stratify at the top of containment, which could significantly reduce the heat transfer rate through the dome and liner.

For the heat transfer analysis provided in Section 2.2.3, the impact of hydrogen is conservatively treated. Any hydrogen in containment is assumed to stratify into a layer consisting entirely of hydrogen in thermal equilibrium with the steam and nitrogen. The steam and nitrogen are still assumed to be well mixed. Given the dimensions of the system, the surface area of the head and liner associated with a volume of stratified hydrogen can be determined. This relationship is illustrated in Figure 3 for the assumed geometry. The ellipsoid shape of the dome causes the rapid decrease in surface area for small additions of hydrogen. For the assumed geometry, there is 166 m^3 of volume above the flange face and 289 m^3 inside the dome and cylindrical section in the cavity region.

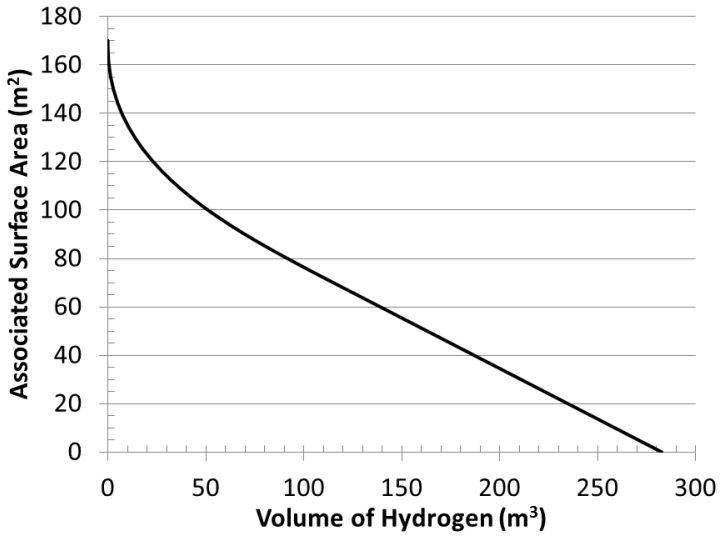

Figure 3. Heat transfer area available versus hydrogen volume stratified in drywell.

2.2.1.2 Basic relationships

The bulk DW pressure, $P_{drywell}$, is the summation of the steam, nitrogen and hydrogen partial pressures, (p_s, p_n, p_h), Eq. (1).

$$P_{drywell} = p_s + p_n + p_h \tag{1}$$

The mass fraction of a constituent, W_i, is given by Eq. (2), where m_i is the mass of a constituent with the subscript indicating the constituent (s = steam, n = nitrogen, h = hydrogen). The mole fraction of a

constituent, x_i, is given by Eq. (3), where N is the number of moles. The summation of the constituent concentrations (mole fractions or mass fractions) is equal to one, as shown in Eqs. (4) and (5).

$$W_i = \frac{m_i}{m_s + m_n + m_h} \tag{2}$$

$$x_i = \frac{N_i}{N_s + N_n + N_h} \tag{3}$$

$$1 = x_s + x_n + x_h \tag{4}$$

$$1 = W_s + W_n + W_h \tag{5}$$

The mole fraction of a constituent can be related to its mass fraction using Eq. (6) for steam and Eq. (7) for hydrogen, where M is the molar mass of the specie (i.e., M_s=18.0153 g/mol, M_n=28.0134 g/mol, M_h=2.0159 g/mol). If the concentration of steam and hydrogen are known, the concentration of nitrogen can be determined using Eq. (4) or (5):

$$x_s = \frac{W_s}{W_s + (1 - W_s - W_h)\frac{M_s}{M_n} + W_h \frac{M_s}{M_h}} \tag{6}$$

$$x_h = \frac{W_h}{W_s \frac{M_h}{M_s} + (1 - W_s - W_h)\frac{M_h}{M_n} + W_h} \tag{7}$$

Through the ideal gas law, the partial pressure of a constituent can be determined through knowledge of the total pressure and the constituent's mole fraction using Eq. (8):

$$p_i = x_i \cdot P_{drywell} \tag{8}$$

When there is a mixture of steam and noncondensables, the bulk temperature in the DW, $T_{bulk,inner}$, is equal to the dry bulb temperature of the partial pressure of steam, as given in Eq. (9):

$$T_{bulk,inner} = T_{sat}(p_s) \tag{9}$$

The mass of the constituents can be determined using the ideal gas law, Eq. (10), for a given containment volume, $V_{containment}$, bulk temperature, and constituent partial pressure, where R_i is the individual constituent ideal gas constant:

$$m_i = \frac{V_{containment} \cdot p_i}{R_i \cdot T_{bulk,inner}} \tag{10}$$

Assuming ideal behavior of the gases, the volume of the stratified hydrogen, V_h, can be determined using the mole fraction and total containment volume as in Eq. (11):

$$V_h = x_h \cdot V_{containment} \quad (11)$$

2.2.1.3 Initial mass of nitrogen in containment

The initial mass of nitrogen in containment can be found as follows. For an assumed initial DW condition of 63°C at 101,325 Pa and 20% relative humidity, the vapor partial pressure is equal to the saturation pressure at 63°C (i.e., 22,887 Pa). The partial pressure of nitrogen, 78,438 Pa, is then found using Eq. (1). (The partial pressure of hydrogen is zero.) The initial mass of nitrogen can then be determined using the ideal gas law as shown in Eq. (10). For a nitrogen partial pressure of 78,438 Pa at 63°C and a containment volume of 4,275 m^3, the initial mass of nitrogen is 4,143 kg.

2.2.2 Heat Transfer Model

Boiling is an extremely effective mode of heat transfer when compared to conduction through the liner and condensation. Therefore, if boiling in the cavity occurs, the outer DW surface will be maintained at approximately the atmospheric boiling temperature (i.e., $T_{w,outer} \approx 100°C$ in Figure 4). To maintain a DW surface temperature of 100°C, the bulk gas temperature inside the DW must be greater than 100°C. When the containment temperature is below 100°C, heat would be convectively removed from the head by overlying water. These two cases for heat transfer through the DW liner and head are illustrated in Figure 4.

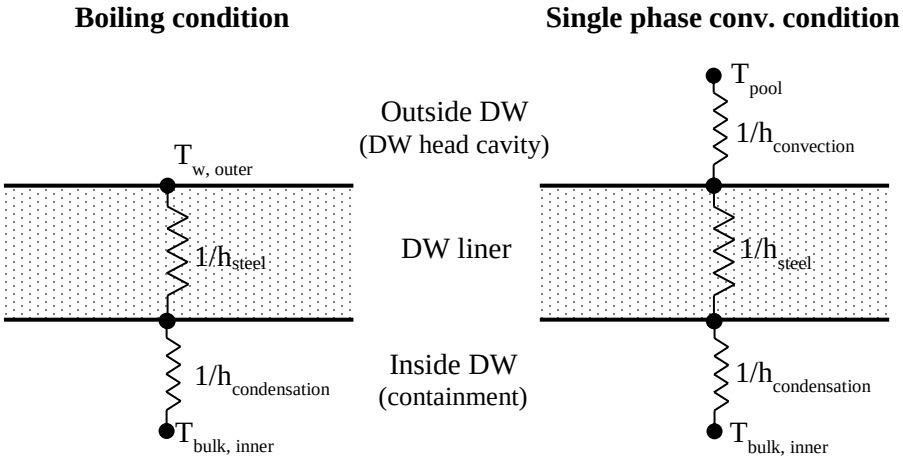

Figure 4. Illustration of heat transfer path and resistances.

In the case of boiling, the heat removal rate, *Q*, through the DW liner and head is given by Eq. (12), where *A*, is the heat transfer area. The heat transfer area is defined as the area of the entire DW head and cylindrical section of liner in the cavity region (170.1 m^2 from Table 3) minus the area associated with any hydrogen present (Figure 3). No heat transfer is assumed to occur through the area associated with the stratified hydrogen. In reality, some heat transfer through this area would occur. This analysis also neglects the heat transfer along the steel liner from the nonstratified to the stratified hydrogen region. The effective heat transfer coefficient, h_{eff}, is given by Eq. (13), where h_{steel} is the effective heat transfer coefficient for conduction across the steel liner, and $h_{condensation}$ is the condensation heat transfer coffeicient at the inside surface.

$$Q = h_{eff} A\left(T_{bulk,inner} - T_{w,outer}\right) \tag{12}$$

$$h_{eff} = 1 \Big/ \left(\frac{1}{h_{steel}} + \frac{1}{h_{condensation}} \right) \tag{13}$$

For cases in which boiling is not occuring, the heat removal rate through the DW liner and head is given by Eq. (14), where T_{pool} is the temperature of the water in the cavity. Again, the heat transfer area is reduced by the area associated with any stratified hydrogen. The effective heat transfer coefficient is given by Eq. (15), where $h_{convection}$ is the heat transfer coefficient for convection on the outer surface. As noted in Table 3, the convective heat transfer rate was assumed to be 30 W/m^2 K for the outer surface. This is a conservative but realistic value. The actual convective heat transfer rate depends on the position and movement of water in the cavity. That is, it depends on water injection, water level, the shape of the cavity, and obstruction by other structures in the cavity. When boiling is not occurring, the temperature of the water in the cavity is assumed to be 40°C. In reality, the temperature of the water depends on the rate of heat and water addition, as well as heat rejection from the pool, or conduction into the surrounding concrete cavity wall and evaporation.

$$Q = h_{eff} A\left(T_{bulk,inner} - T_{pool}\right) \tag{14}$$

$$h_{eff} = \frac{1}{\left(\frac{1}{h_{convection}} + \frac{1}{h_{steel}} + \frac{1}{h_{condensation}}\right)} \tag{15}$$

The effective heat transfer coefficient due to conduction across the DW liner is given by Eq. (16), where k_{steel} is the conductivity of the steel, and δ is the liner/head thickness.

$$h_{steel} = k_{steel} / \delta \tag{16}$$

The condensation heat transfer coefficient as a function of noncondensable mass fraction is given by the Uchida [17] correlation in Eq. (17). It has been noted that the Uchida correlation can overpredict heat transfer at containment pressures below 1 bar, and it can underpredict heat transfer at containment pressures above 1 bar [18].

$$h_{condensation} = 380 \left(\frac{W_n}{1 - W_n}\right)^{-0.7} \ (\mathrm{W/m^2 - K}) \tag{17}$$

The heat transfer rate is taken as the maximum between the heat transfer rates for the external condition of boiling or convection.

2.2.3 Heat Transfer Results

Using the heat transfer model discussed, the results from Sections 2.2.1, and the assumed parameters in Table 3, the total heat transfer rate can be determined as a function of containment pressure (i.e., for a given hydrogen and steam partial pressure).

Two cases are discussed below. For the constant nitrogen mass case discussed Section 2.2.3.1, the mass of nitrogen in the DW is assumed to remain constant and equal to the initial amount. For the variable

nitrogen case discussed in Section 2.2.3.2, the amount of nitrogen is allowed to vary, and the heat transfer rate is determined for various steam and hydrogen concentrations.

2.2.3.1 Constant nitrogen mass

For this case, the mass of nitrogen in containment is assumed to remain constant. With this assumption and the geometry specified in Table 3, the heat transfer rate can be determined as a function of containment pressure and mass of hydrogen.

Results with no hydrogen present are presented in Figure 5 and Figure 6. While the containment temperature is below approximately 100°C, the heat transfer rate is <300 kW. This is as expected, as the containment temperature is not sufficient to cause the overlying water to boil, and the heat transfer resistance via single phase convection is high. At containment pressures above ≈0.25 MPa, the steam partial pressure is sufficient to result in containment temperatures above 100°C. At these conditions, the heat removal rate greatly increases with containment pressure. At a design pressure of 0.42 MPa (56 psig), the heat removal rate is 2.1 MW. At 0.87 MPa (112 psig) the heat removal rate is 6.2 MW.

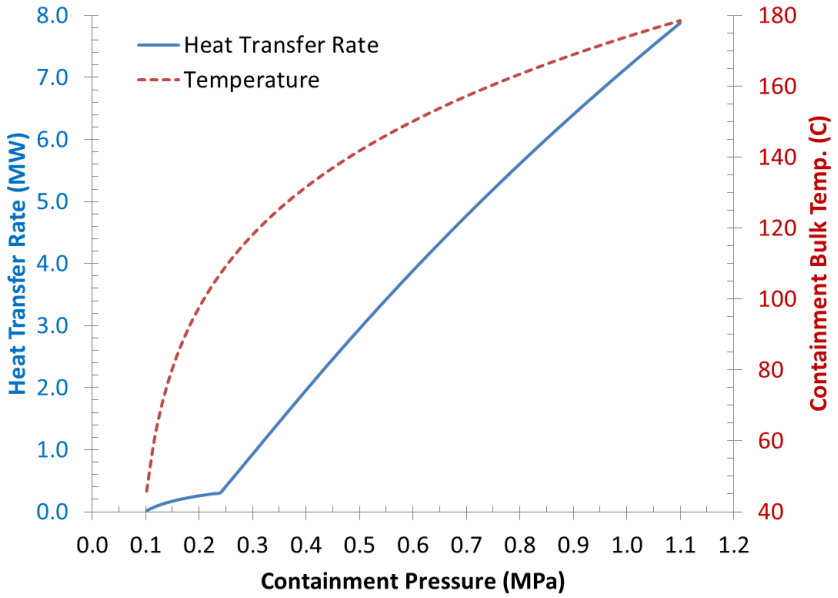

Figure 5. Heat transfer rate and containment temperature vs containment pressure: no hydrogen.

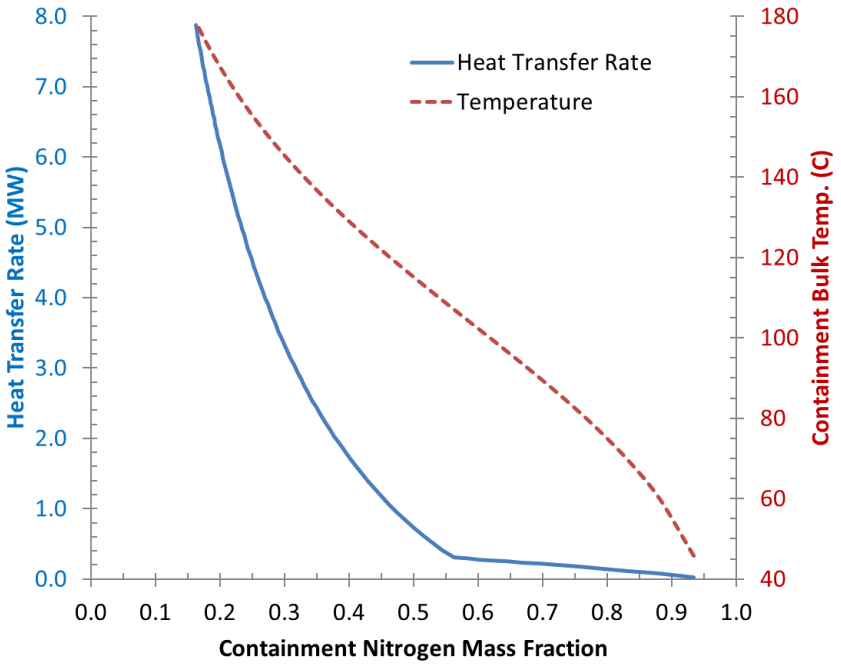

Figure 6. Heat transfer rate and containment temperature vs mass fraction of nitrogen: no hydrogen.

With hydrogen present and assumed to be stratified at the top of the DW, the area available for heat transfer decreases. Figure 7 illustrates the heat transfer area available for various containment pressures and masses of hydrogen in containment. As expected, increasing the amount of hydrogen reduces the amount of heat transfer surface area. Also, for a given mass of hydrogen, as the contain increases in pressure, the hydrogen is compressed, and the heat transfer area increases.

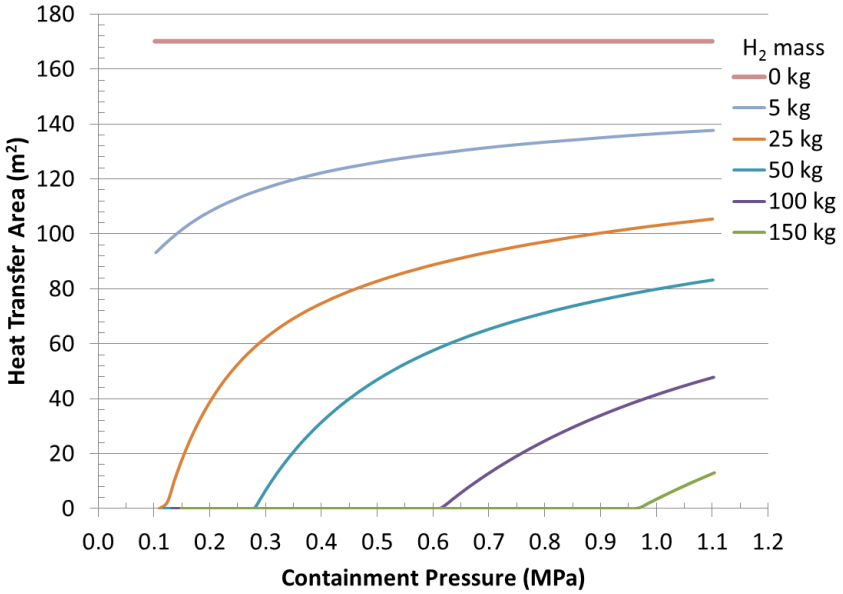

Figure 7. Reduction in heat transfer area due to hydrogen vs containment pressure.

With a reduction in the heat transfer area, the overall heat transfer rate decreases with increasing hydrogen mass in containment, as seen in Figure 8. The amount of hydrogen that may be generated during a severe accident can be over 1,000 kg. Therefore, given the assumption of hydrogen stratification and the other assumptions noted in Section 2.2, relatively small amounts of hydrogen in containment readily deteriorate the potential heat transfer through the DW head region.

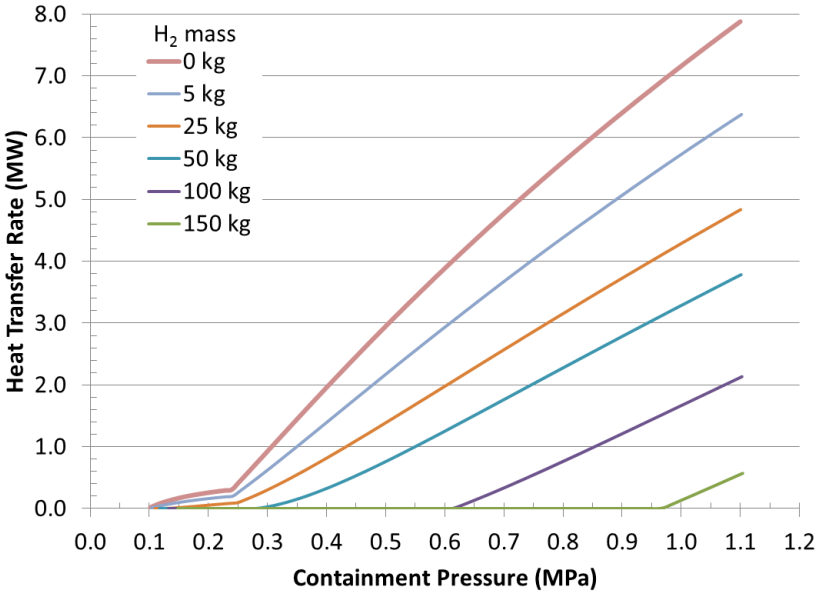

Figure 8. Heat transfer rate vs containment pressure with various amounts of hydrogen.

2.2.3.2 Variable nitrogen

For this case, the mass of nitrogen in containment is allowed to vary. For a given DW pressure mass fraction of steam and hydrogen, the mass fraction of nitrogen can be determined using Eq. (5). The related mole fractions can be determined using Eqs. (6), (7), and (4). With the DW pressure and mole fraction of steam known, the partial pressure of steam can be determined using Eq. (8). The bulk temperature can then be determined using Eq. (9). The volume of the stratified hydrogen is determined using Eq. (11) and is related to the DW head surface area through geometry (Section 2.2.1.1). The heat transfer rate can then be determined as a function of containment pressure using the relation given in Section 2.2.2.

The results with no hydrogen present are presented in Figure 9 and Figure 10. The mass fraction of steam (or conversely the mass fraction of nitrogen) has a large impact on the heat transfer rate. Early in the accident sequence when the containment is a low pressure and is mostly filled with nitrogen, the potential heat transfer through the DW head is quite low (i.e. less than 200kW). As the accident progresses, the DW pressure will increase and the concentration of steam in containment will increase. Both of these factors will enhance heat removal through the DW head. There is the potential for substantial heat removal (i.e., multi-MW) at high steam mass fractions.

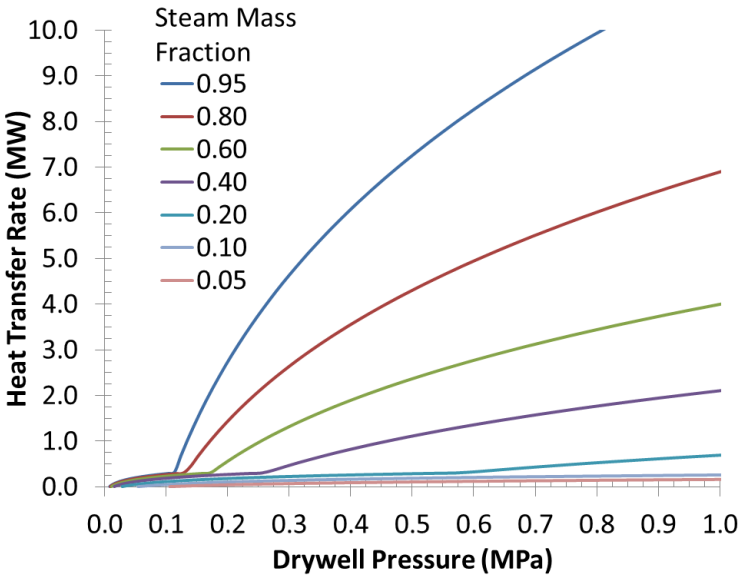

Figure 9. Heat transfer rate vs drywell pressure for various steam mass fractions: no hydrogen.

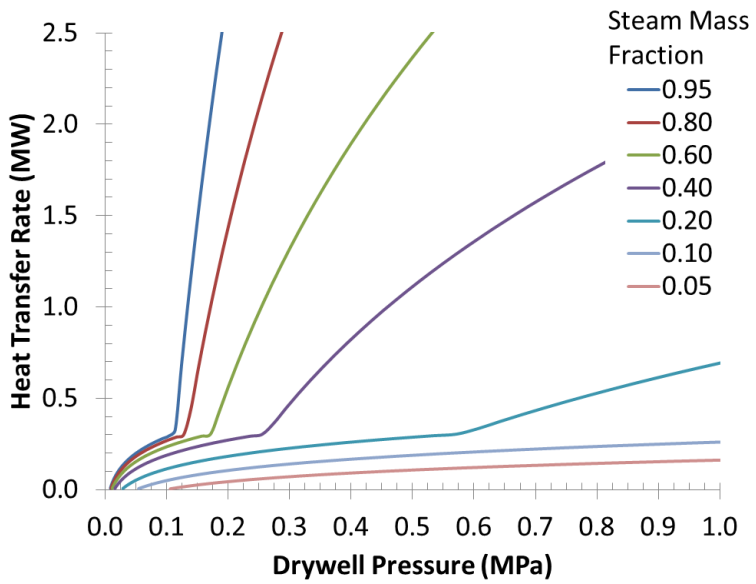

Figure 10. Heat transfer rate vs drywell pressure for various steam mass fractions: no hydrogen, expanded view.

The heat transfer through the head has been correlated in the forms of Eqs. (18–20), where Q_{boil} and Q_{conv} are the convective regime and boiling regime heat transfer rates, respectively. The heat transfer rates are in units of MW, and the DW pressure is in units of MPa. A comparison of the correlated model (i.e. Eqs. 18-20) to the results of the analytical model (i.e. Eqs. 4-9 and 11) is provided in Figure 11.

$$Q_{conv} = \left(0.0104 \cdot \ln\left(W_s\right) + 0.1142\right) \cdot \ln\left(P_{drywell}\right) + \left(0.1251 \cdot \ln\left(W_s\right) + 0.5462\right) \tag{18}$$

$$Q_{boil} = \left(9.5213 \cdot W_s^{\,4} - 8.8008 \cdot W_s^{\,3} + 1.5463 \cdot W_s^{\,2} + 3.4961 \cdot W_s\right) \cdot \ln\left(P_{drywell}\right) + \ldots \left(35.0068 \cdot W_s^{\,4} - 51.7334 \cdot W_s^{\,3} + 30.421 \cdot W_s^{\,2} - 0.9648 \cdot W\right) \tag{19}$$

$$Q = \max\left(Q_{conv}, Q_{boil}\right) \tag{20}$$

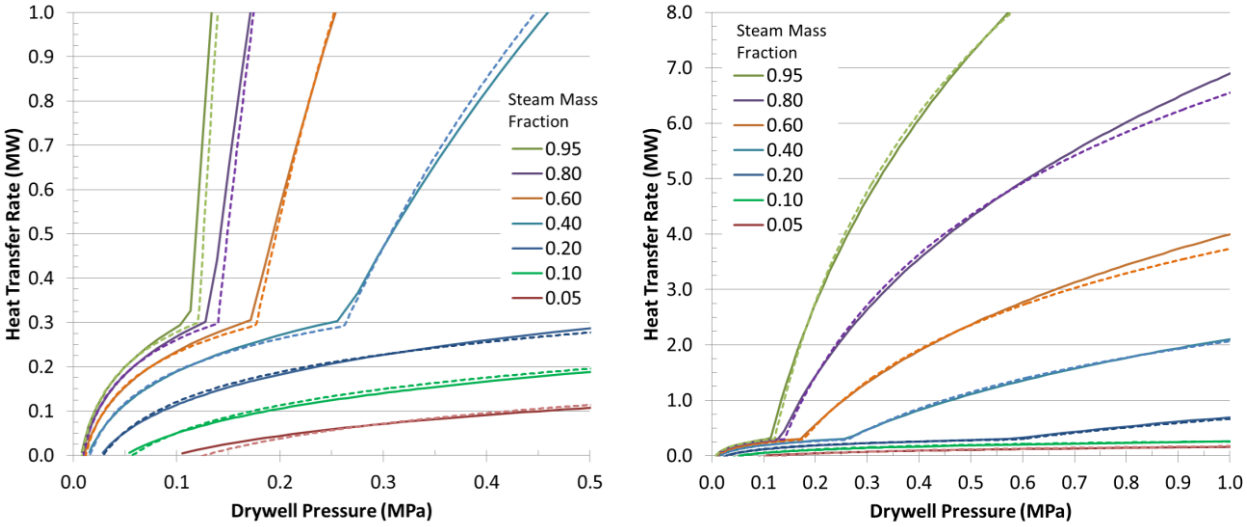

Figure 11. Comparison of correlated (dashed lines) to analytical model (solid lines) heat transfer.

As noted previously, with hydrogen present and assumed to be stratified at the top of the DW, the area available for heat transfer decreases. Figure 12 provides the heat transfer results for a range of DW pressures, steam mass fractions, and hydrogen mass fractions. Relatively low masses or concentrations of hydrogen substantially reduce the efficacy of heat transfer through the DW head. For example, at 1 MPa, 0.40 steam mass fraction, and 0.0050 hydrogen mass fraction, the corresponding hydrogen mass is ≈132 kg. During an accident, once hydrogen production accelerates, the potential heat removal through the DW head will greatly diminish. However, these results are predicated on the assumption of hydrogen stratification in the DW.

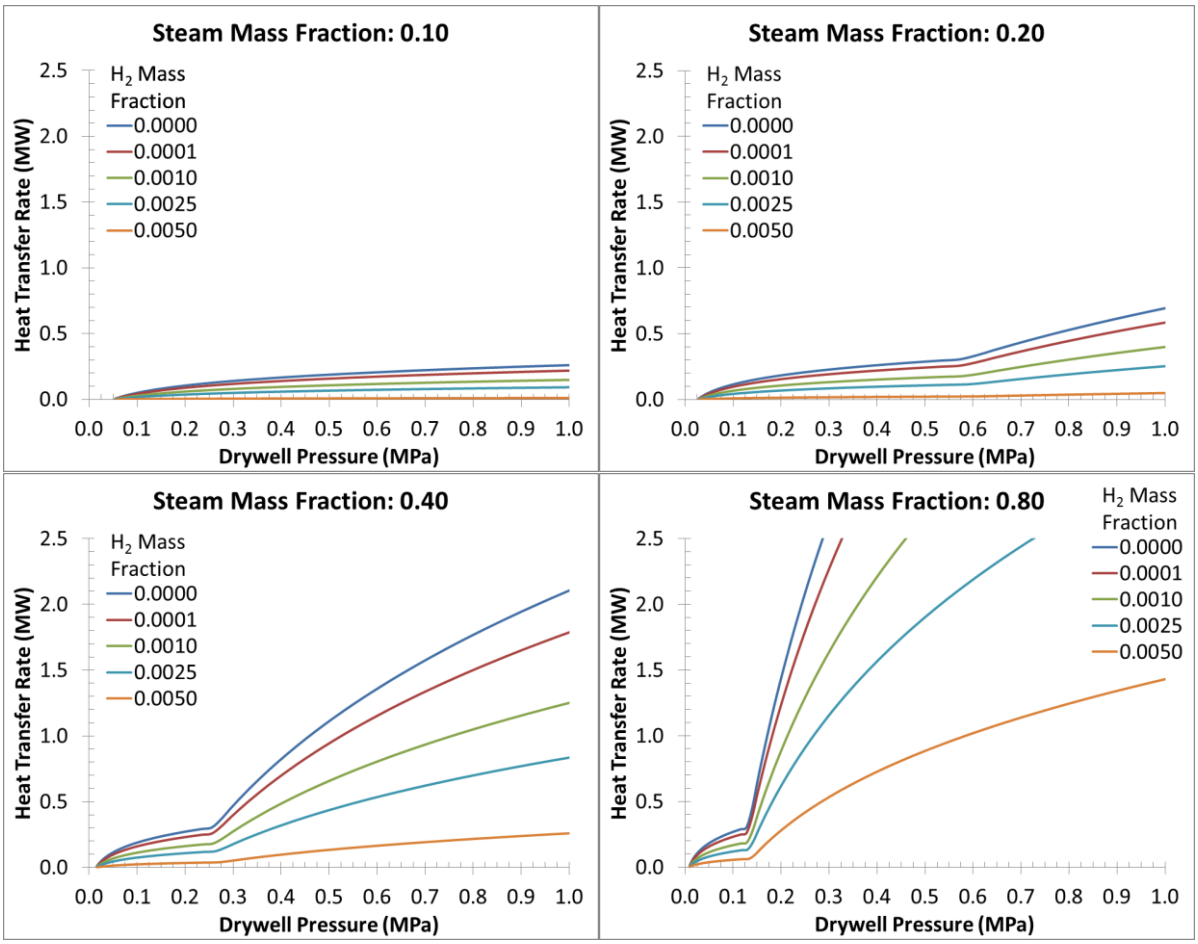

Figure 12**. Effect of hydrogen on the heat transfer rate for various steam mass fractions.**

2.3 WATER INVENTORY AND MAKEUP

To completely fill the cavity with water with the DW head in place (DW head cavity shown in Figure 1) would require 342 m^3 (90,375 gal) of water. To fill the cavity up to the top of the DW head would require 254 m^3 (67,214 gal) of water. Table 4 specifies the time required to fill the cavity to the top of the DW head for various pumping capacities and assuming no inventory losses from boiling, for example.

Table 4. Time to fill cavity vs pumping capacity

Water injection rate (lpm)	Water injection rate (gpm)	Time to fill cavity to top of DW head (h)
379	100	11.2
757	200	5.6
1,893	500	2.2
3,785	1,000	1.1
9,464	2,500	0.4
18,927	5,000	0.2

Water injection may be required to offset the inventory loss due to boiling. Assuming that water is injected at 25°C and boils at atmospheric pressure, the rate of water injection to offset the heat removal rate is shown in Figure 13 for the case of no hydrogen present (from Section 2.2.3).

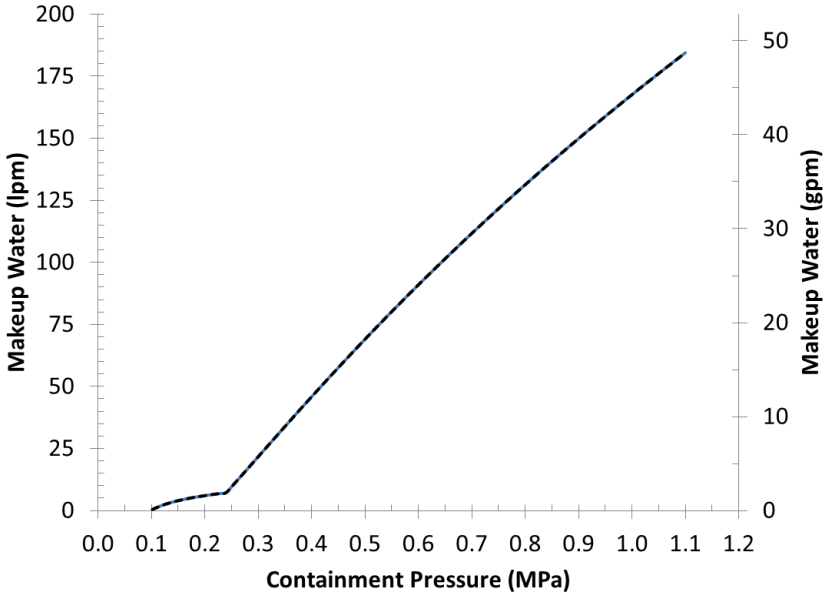

Figure 13. Makeup water required to offset inventory loss due to boiling.

To initially fill the cavity in a reasonable amount of time, a flow rate of ~2,000 lpm (~500 gpm) may be required. However, it is important to note that the cavity may not need to be filled since the injected water would contact the DW head and liner, thus removing heat. To offset the losses due to boiling over the long term, a relatively low amount of water injection is required <200 lpm (<50 gpm). While onsite equipment can vary between sites, these injection rates are quite reasonable and are also within the general capabilities of the FLEX equipment.

2.4 FLANGE LOADING DISCUSSION

The DW head flange design can vary between units (e.g., number and length of bolts). However, they all include pretensioned bolts that maintain loading on the sealing surface. As the DW pressurizes, this preload is offset. With sufficient pressure, the bolts can elastically stretch, forming a gap at the flange seal. Depending on the type of seal, the gasket material can rebound a certain percentage of its preloaded dimensions. If a gap forms greater than the rebounded seal material, leakage through the flange will commence.

The DW head, bolts, and seal temperatures (both the magnitude and differentials) can all affect the integrity of the flange seal. As the temperature of the bolts increases, their elastic modulus decreases. For the same applied force (i.e., DW pressure) the bolt strain increases with increasing temperature. Elastomeric seals can be degraded or extruded at elevated temperature and pressures. As the DW head is pressurized, it applies various loads to the sealing surface (e.g., bending moments). This loading is affected by differential thermal expansion and temperature-dependent material properties.

Injecting water into the cavity would have two effects on the seal's integrity. First, the water would cool the bolts, limiting their loss of pre-tension due to thermal expansion and creep. The water would also cool the seal material and the DW head. Second, the pressure from any accumulated water in the cavity could offset some of the loading due to DW pressurization. Of these two effects, the first is likely to have the most impact.

2.5 SCRUBBING CAPABILITY AND REFUELING BAY ENVIRONMENT DISCUSSION

Water pools can remove or scrub aerosols and vapors from injected gas. The suppression pool in the Mark I and II containments' wetwell can condense steam and scrub fission products. As in the suppression pool, if the DW head cavity were flooded, leakage through the DW head flange seal could condense steam and scrub fission products before being released to the refueling floor and ultimately the environment.

Fission product scrubbing involves a range of phenomena with respect to thermal-hydraulics, including bubble breakup, coalescence, condensation, shape, rise velocity, etc. It also involves aerosol physics, including Brownian diffusion, impaction, deposition, settling, chemistry, etc. Codes such as SPARC 90 [19] model these phenomena to varying degrees to simulate the ability of water pools to scrub aerosols. MELCOR relies on the SPARC-90 models—in coordination with the control volume hydrodynamics package and MAEROS models for aerosol dynamics—to predict aerosol and iodine vapor scrubbing.

Despite the complicated physics, three factors have been identified that may differentiate the ability of water in the DW head cavity region to condense steam and scrub fission products compared to water in the suppression pool. The terminal ends of the downcomer vent pipes, the safety relief valve (SRV) spargers, and high pressure coolant injection system (HPCI) and reactor core isolation cooling system (RCIC) tail pipes are approximately 1.3–3.2 m below the suppression pool's surface. Depending on the amount of water in the DW head cavity, the DW flange could be submerged up to 4.4 m (Section 1.3). Thus, the DW head cavity region and the suppression pool have comparable water depths. Over the course of an accident, the suppression pool temperature increases, while its ability to condense steam and scrub fission products decreases. Similar effects may occur in the flooded DW head cavity region. Finally, the size of the downcomer vent pipes, the SRV spargers, and HPCI and RCIC tail pipes are of known sizes. The orifice through which the gases are injected into the pool is designed. The leak path characteristics of the DW head flange are not known. As mentioned in Section 1.4.2, an average flow area of approximately 5 cm^2 is predicted for simulations of the events at 1F1, which is fairly small. Differences in the flow area, characteristic length, and flow rate confound the comparison of scrubbing efficacy between the suppression pool and water in the DW head cavity.

3. INTEGRAL ANALYSIS SIMULATIONS SETUP

The effects of the proposed accident mitigation action during accidents is simulated in Section 4. This section describes the accident scenarios chosen, the figures of merit used in the comparison, the MELCOR code, the plant model, and the modeling of the DW head and cavity region. Information provided in Sections 3.2 and 3.3.6 has been reported by Robb and Howell 2017 [20] and is provided here for the ease of the reader.

3.1 ANALYSIS FIGURES OF MERIT

Key figures of merit, provided in Table 5, are defined related to the timing of the accident progression and potential scrubbing.

Table 5. Figures of merit descriptions

Figure of merit		Significance
Timing	DW reaches 0.49 MPa (56 psig)	DW design pressure
	Containment failure	Loss of radionuclide barrier
	First deflagration in building	Escalation of accident
	0.5 kg of noble gas release to environment	Onset of radionuclide release to outside
Fraction released to environment by end of simulation	Class 2, 4, 6 (Cs, I, CsI, ...) to environment	Impacts off-site consequences
	Class 3 (Sr, Ba, ...) to environment	Impacts off-site consequences

3.2 OVERVIEW OF TOOLS

MELCOR is a system-level code that models the progression of severe accidents in light water nuclear power plants [16]. It was developed and has been maintained by Sandia National Laboratories for the NRC. The code encompasses various phenomena that can occur during a severe accident, including the thermal-hydraulic response; the heat up, degradation and relocation of the core material; transport of radionuclides; and hydrogen generation and combustion. MELCOR is primarily used to estimate the source term from postulated severe accidents. In this study, MELCOR version 1.8.6(.4073), as compiled by ORNL personnel using the Intel 11.1.064 compiler, is used on a Linux-based computer with Intel-based hardware.

3.3 PLANT MODEL

3.3.1 Overview

The MELCOR plant model used is for Peach Bottom (Unit 2 or 3), a BWR series 4 (BWR/4) with Mark I containment. The model is the same as that used in previous analyses [20] except for the changes noted in this section. The model incorporates all major components, including the reactor, containment, reactor building, various cooling systems (pumps, sprays, piping, tanks), and system and scenario control logic. The model's lineage and additional model updates are described in Robb 2014 [21].

The BWR/4 with Mark I containment includes a number of key systems that interplay during an accident. The RCIC and HPCI systems are steam-driven pumps that can inject water into the RPV. Without other water injection (i.e. from systems relying on alternating current [AC] power or alternate external systems), the RCIC and HPCI systems are used during station blackout as long as direct current [DC] power remains. These systems have various trip settings, including net positive suction head limits and

low steam line pressure. The SRVs are located on lines coming off of the main steam lines that can vent steam from the RPV to the suppression pool. The suppression pool (aka suppression chamber) is a large water pool located in the torus or wetwell vessel near the bottom of the Mark I containment. Without access to an external ultimate heat sink due to loss of AC power or other events, this pool serves as the heat sink to condense steam being released from the RPV. The rate of containment pressurization is slowed by condensing this steam. However, once the suppression pool reaches saturated or near saturated conditions, its capability to condense steam is thwarted, and the rate of containment pressurization increases. The suppression pool can also scrub fission products released from the RPV.

Within the model, there are different competing failure modes for various structures in the system. Minor differences in accident progression (i.e., minor differences in pressure) can result in different failure modes, causing simulations to vary substantially from one another.

Three competing modes are modeled for lower head failure: thermal failure of a penetration caused by the high temperature of a penetration or the lower head, lower head yielding via creep-rupture, and RPV over-pressurization. Because RPV over-pressurization will not occur during the accident scenarios selected, competition is only between the failure of a penetration due to high temperature and yielding of the lower head.

Four competing failure modes are modeled for the containment. Three are functions of pressure and local temperature and include rupture of the wetwell, rupture of the DW liner, and leakage of the DW head flange (Section 3.3.4). The fourth mode is melt-through of the DW liner from contact with molten core materials. Each failure mode opens different release paths through which radionuclides and combustible gases pass into the reactor building.

3.3.2 Modeling Heat Transfer through DW Head Region

For the simulations described in Section 4, two different methods of modeling the heat transfer through the DW head were examined.

3.3.2.1 Parametric heat transfer model

This model relies on the correlated heat transfer, as specified in Eqs. (18–20) presented in Section 2.2.3.2. In these relations, the heat transfer is a function of DW pressure and steam concentration. As noted in Section 2.2.3, the addition of hydrogen, which is assumed to stratify, greatly reduces the heat transfer. This effect is captured pragmatically by preventing heat transfer through the DW head region—as predicted by Eqs. (18–20)—if more than 10 kg of hydrogen is present in containment. This method uses the base model DW discretization noted in Section 3.3.3.1. The heat transfer through the DW head region is removed from the DW atmosphere and applied to the water in the DW head cavity.

3.3.2.2 Integrated physics heat transfer model

This model relies on the models incorporated in MELCOR for heat transfer (condensation, conduction, and convection) and mass transport (gas concentrations). The default values for the various model parameters were used (MELCOR sensitivity coefficients). This method uses the refined model DW discretization noted in Section 3.3.3.2.

Heat transfer through the DW head could be enhanced with the inclusion of fins or other features. The impact of the DW head heat transfer area was investigated parametrically by increasing both the inside and outside surfaces by a factor of 3× from 102.9 m^2 to 308.7 m^2. This increased the total heat transfer area, including the dome and cylindrical portions of the DW head, by a factor of 2.2× from

170.1 m^2 to 375.9 m^2 (values for inside surface). This is a simple approach to investigate whether enhancing the DW head heat transfer area has an appreciable impact on the passive heat removal capability of the DW.

3.3.3 Drywell Discretization

The simulations described in Section 4 include two different DW discretizations, a simple basic model and a higher fidelity refined model.

3.3.3.1 Basic model

For the basic model, the DW consists of two control volumes (CVs). One CV encompasses the space inside the pedestal region below the RPV (105 in Figure 14). The other CV includes the space outside the pedestal (encompassing 100, 101, 102, 104 in Figure 14). In addition to these two CVs, each of the eight DW-to-wetwell vents is modeled with their own CV. The elliptical DW head is modeled with 1 heat structure. Another heat structure models the cylindrical portion of the DW head, starting 1 m below the flange.

3.3.3.2 Refined model

For the revised DW model, termed the "refined model," the discretization of the DW CVs and heat structures were increased, and additional flow paths between volumes were created.

The single DW CV external of the RPV pedestal was divided into four CVs. The control volumes of the DW are illustrated in Figure 14.

- CV 100 includes the lower portion of the DW.
- CV 101 covers the middle section of the DW.
- CV 102 is located at the transition between the DW liner and the cylindrical portion of the DW head region. The base of CV 102 corresponds to the base of the CV external of the DW head (CV 411).
- CV 104 models the annular space between the RPV and the concrete biological shield.

The total volume of the DW in the refined model is the same as that in the base model. The division of the DW into CV 100, 101, 102, and 105 is similar to that previously explored in the State of the Art Reactor Consequence Analysis (SOARCA) study [22]. Accounting for the flow path between the RPV and biological shield (CV 104) was previously considered in a GOTHIC analysis of the Mark I containment [23].

Six flow paths were created connecting the various control volumes. A flow path can only model gaseous flow in one direction at any given time. Therefore, to capture the possible natural circulation paths within the DW, two flow paths were defined to connect CV 100 to CV 101. The flow path heights were slightly offset. In addition, two flow paths were created to connect CV 101 to CV 102. Two additional flow paths connected CV 104 to CV 105 and CV101.

In MELCOR, each surface of a heat structure must lie entirely within a control volume. Due to the increased discretization of the DW, the heat structures representing the biological shield, main steam lines, and miscellaneous steel in the DW were subdivided.

In addition to these changes, the film tracking model for condensation heat transfer was added to appropriately pass the liquid film from the biological shield to the lower pedestal walls.

The two heat structures for the DW head and cylindrical section below the head were modified to reflect the geometry assumed in Section 2.1. The cylindrical section was modeled using MELCOR's option for cylindrical surfaces. MELCOR does not include an option to model the elliptical shape of the DW dome. Therefore, the dome was modeled as a rectangular surface that conserves the surface area. This heat structure was slightly inclined at 14 degrees.

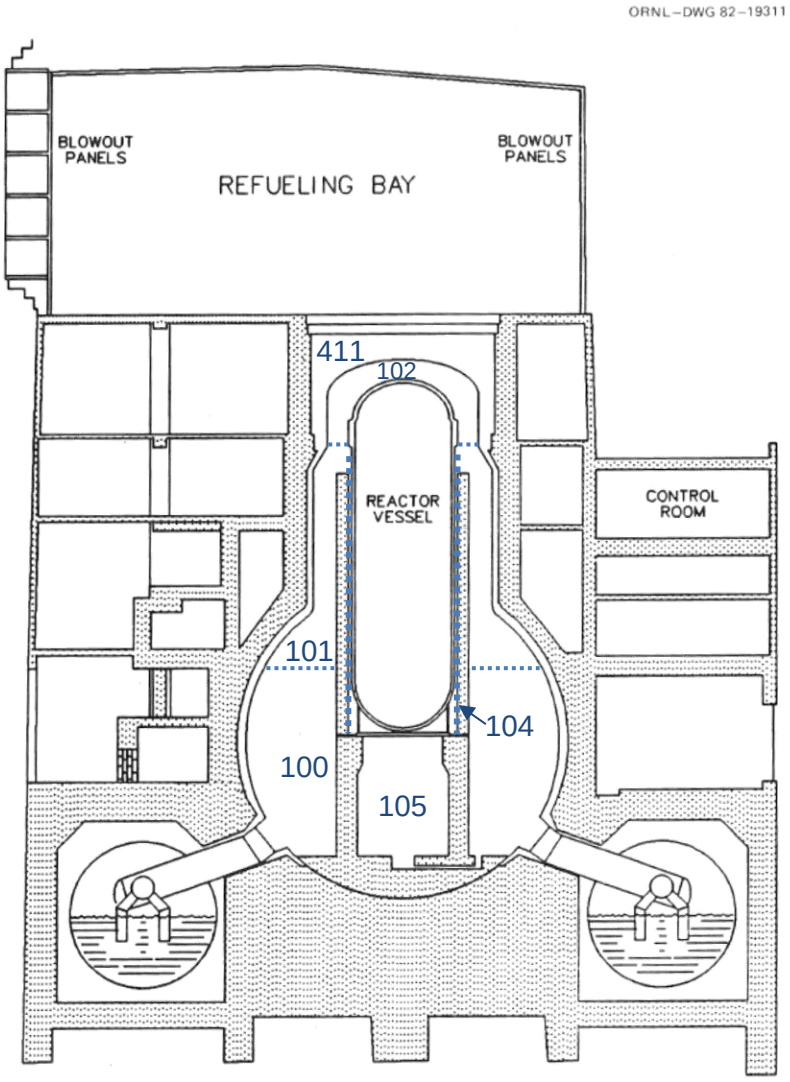

Figure 14. DW discretization for refined model.

3.3.4 Drywell Head Failure Modes

For the studies presented in Section 4, two DW head flange seal leak models were incorporated and used. The following sections describe these two models. Development and/or validation of DW head leakage models are beyond this work scope. Development of a holistic model that accounts for thermal and pressure effects is an area for future work.

3.3.4.1 Temperature and pressure (T&P) limit model

In the assumed temperature and pressure (T&P) limit model, the DW head flange failure mode forms a 0.03 m^2 flow path through the DW head flange seal based on temperature versus pressure criteria (Table 6 and Figure 15). For temperatures between the values provided in Table 6, a linear interpolation is performed to determine the failure pressure. Once the criterion is exceeded, the 0.03 m^2 leakage flow path forms and remains open for the remainder of the simulation. While this model takes temperature into account, leakage could occur for some gasket materials (e.g., EPDM) before reaching such high temperatures.

Table 6. T&P limit DW head leakage model

DW head flange temperature (K)	Failure pressure (kPa-gauge) (psig)	Leakage area (m^2)
≤450.0	965.3 (140)	0.03
644.2	689.5 (100)	0.03
≥755.6	34.5 (5)	0.03

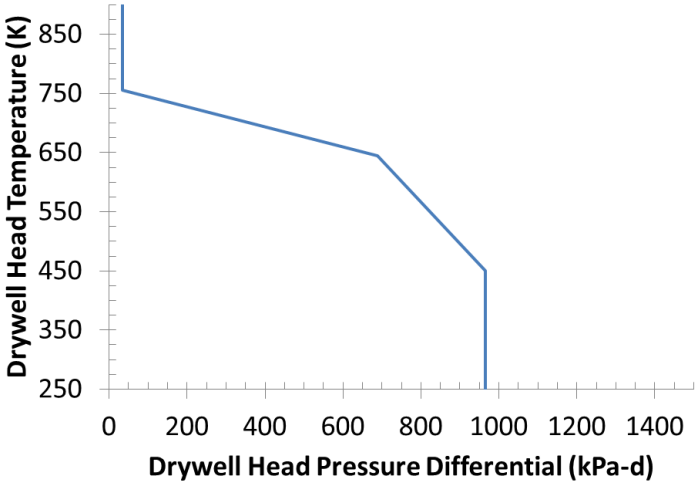

Figure 15. DW head flange seal pressure vs. temperature failure criteria.

3.3.4.2 Variable leak area model

This leakage model, termed the *variable area model*, is derived from the SOARCA for the Peach Bottom Nuclear Power Station, for which a variable DW head flange seal leak was modeled as a function of DW pressure [22,24]. The relationship from Mattie et al. [24] is shown in Figure 16. The relationship is derived using simple mechanical loading analysis of the DW head flange accounting for the size, number, and pre-tension of the bolts, as well as gasket recovery. As the DW pressurizes, the DW bolts stretch, elastically forming a leak path through the flange seal. This model does not take DW head flange, bolting, gasket material temperature, or temperature-driven degradation into account.

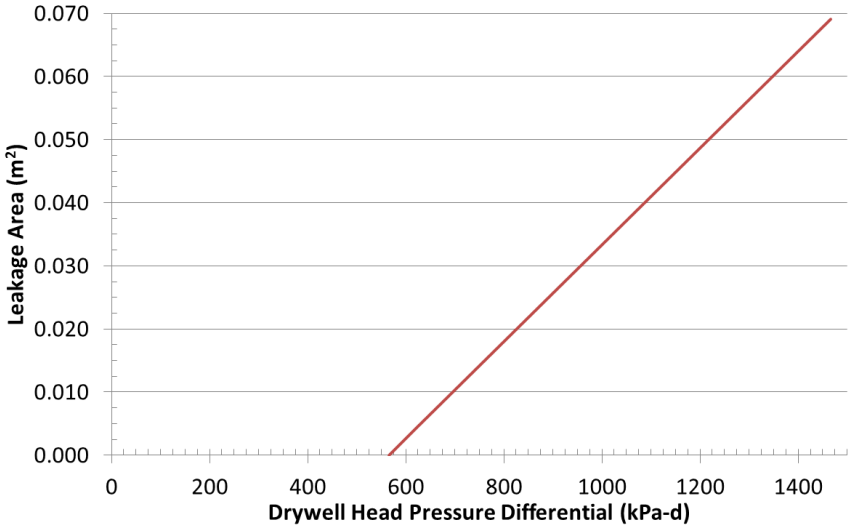

Figure 16. DW head flange seal leak flow area vs pressure.

As noted in Section 1.4.2, the DW pressure of Fukushima Daiichi Unit 1 is reproduced by modeling a DW head leakage flow area of approximately 4.5–7.5 cm^2. This is on the order of 50 times lower than the leak area assumed to be formed (0.03 m^2) by the pressure- and temperature-dependent failure model. The 4.5–7.5 cm^2 leak area range is also approximately 10 times lower than would be predicted by the pressure dependent model used in SOARCA. The baseline model is shown in Figures 4.1–19 in Mattie et al. [24].

3.3.5 Primary System Leakage

3.3.5.1 Background

During a station blackout accident, there are a few potential pathways for leakage from the primary system into the DW. These possible paths include paths through the SRV flange seal, the primary recirculation pump seals, the creep-rupture of a main steam line, and others. Leaking liquid water or steam would directly introduce steam into the DW atmosphere, increasing the pressure and steam concentration. Liquid water would flash, depending on the conditions).

The reactor coolant pump (RCP) seals may leak under typical operating conditions and experience enhanced leakage during off-normal conditions. The potential for the RCP seals to leak during a station blackout and the potential leak rate was discussed in detail during resolution of NRC Generic Safety Issue 23 (GSI-23) [25]. With respect to GSI-23, BWRs are not included in the scope due to the following:

> *seal failures in BWRs result in smaller leak rates than seal failures in PWRs. Additionally, seal failures in BWRs may be mitigated by the recirculation loop isolation valves, and the reactor coolant makeup capability of the reactor core isolation cooling system, the high-pressure coolant injection system, and the feedwater system is greater in BWRs than is the capability of comparable makeup systems in PWRs* [25].

Work during the GSI-23 process indicated a maximum leak rate (per RCP) of 100 GPM, with 18 GPM assumed nonfailure leakages [26].

During the assessment of the events at Fukushima Daiichi, the DW pressurization for 1F3 was higher than would typically be predicted by the MELCOR and MAAP codes [10,12]. One possible cause for the increased pressurization was attributed to leakage of the RCP seals [12,27], while another cause was attributed to thermal stratification and possible local saturation of the suppression pool [10]. In one study,

an RCP leakage rate of 1 kg/s (2 kg/s total for two pumps) was assumed [12], while another study assumed a leakage flow area of 0.55 cm^2 (yielding leak rates ≤5.5 kg/s) [27]. As noted in Section 2.2.3, the potential heat removal through the DW head depends the DW pressure and steam concentration. Leakage of water through the RCP seals and subsequent flashing affects the DW pressure and steam concentration.

3.3.5.2 RCP leakage model

An option was added to simulate leakage from the primary system into the DW. Two flow paths were added simulating leakage through the RCP seals (one flow path for each pump). The flow path was assumed to be 25.4 mm long and 5.16 mm in diameter. This leak size was chosen to produce a leak rate of approximately 1 kg/s (through each RCP) while the RPV is at normal operating pressure. For simulations using this model, the leak was assumed to start 600 s after reactor shutdown. MELCOR calculates the potential flashing of the leaking coolant into the DW atmosphere.

3.3.6 Other Recent Model Modifications

Two additional changes were recently made to the model with regard to HPCI operation and operator actions to depressurize the RPV [20], as discussed below.

3.3.6.1 Operator RPV depressurization action

In previous studies of the Peach Bottom model, operators took action to depressurize the reactor by opening an SRV if the suppression pool reached a predefined heat capacity limit. However, as modeled, the operators would depressurize the reactor to a point below which the RCIC and HPCI systems would trip from low steam pressure. This could result in early isolation of the RCIC and HPCI. In reality, however, operators took action to depressurize the reactor, but they maintained sufficient steam pressure to allow for continued operation of the RCIC or HPCI.

The logic in the MELCOR model was modified to prevent operators from depressurizing the RPV below the isolation trip point of the RCIC and HPCI because of low steam pressure. This enables extended operation of the RCIC and HPCI systems.

3.3.6.2 HPCI actuation logic

The models for the RCIC and HPCI operation previously contained logic that could cause both systems to actuate (i.e., turn on and off) at the same time. This resulted in cyclic periods of large steam draw and rapid refill of the RPV. In reality, operators can take action to use one system or the other at any given time. An additional user option was added to the model to prevent HPCI operation while the RCIC is available for operation. This option prevents the RCIC and HPCI systems from operating at the same time.

3.3.7 Note on Wetwell Discretization and Physics

The wetwell is a large torus structure into which steam is vented from the SRVs, RCIC, HPCI, and DW-to-wetwell vents. Certain thermal hydraulic phenomena such as local saturation, thermal stratification, and local and global circulation can impact the performance of the wetwell [28]. MELCOR's ability to accurately capture these phenomena in the wetwell is limited and dependent on wetwell discretization [10,29]. The MELCOR model employed uses eight control volumes to represent the wetwell. Each DW-to-wetwell vent is also modeled with its own control volume. Further description of the model is provided in Robb 2014 [21]. While the model is more refined than using a single control

volume to represent the large wetwell, modeling of the wetwell likely impacts the predicted containment pressurization response and subsequently the assessment of the drywell head cooling mitigation action.

3.3.8 Note on Ex-Vessel Modeling

The core-concrete interaction modeling in MELCOR is performed using a separate package that is based on CORCON-Mod3 with its own material properties. Limited ex-vessel debris coolability models are integrated into the released MELCOR 1.8.6 and 2.1 versions [16,30].

3.4 ACCIDENT SCENARIO AND CASES

Two accident scenarios were chosen for investigation: a long-term station blackout (LTSBO) and an extended loss of AC power (ELAP).

3.4.1 Long-Term Station Blackout Accident Scenario

The LTSBO is one variant of a station blackout (SBO). An SBO scenario was chosen for analysis due to its high contribution to the overall core damage frequency for BWRs [22,31]. Furthermore, the accidents which occurred at Fukushima Daiichi Units 1–3 were SBO variants [3].

For the LTSBO scenario, the reactor is assumed to successfully trip (reference time 0 h). All AC power, including off-site and onsite AC power from diesel generators, is assumed to be lost at 0 h. The timing of the loss of DC power from batteries was modeled to occur at 8 h. While DC power is maintained, the RCIC and HPCI systems can be used to inject cooling water into the primary system. As modeled, operators do not control the speed of the RCIC or HPCI systems. Thus, they turn full-on and off as necessitated by the water level. Also, as modeled, these systems are aligned to take suction from the condensate storage tank. Steam generated in the RPV is vented through the RCIC, HPCI, or SRVs. Manual operation of the SRVs relies on DC power and plant air availability. As modeled, the operators use an SRV to manually depressurize the RPV down to approximately 1.14 MPa (150 psig) if the suppression pool exceeds its heat capacity limit. Once DC power is lost, the ability to manually actuate the SRVs is lost, and the RPV can repressurize up to the pressure set point for automatic SRV actuation.

After DC power failure, water injection into the primary system ceases and is assumed not to be restored. After water injection ceases, the reactor pressure vessel water inventory boils away, uncovering the core. The fuel rods heat up, oxidize, generate heat and hydrogen, and begin to fail. The failed fuel relocates downward and may eventually fail the lower head of the RPV. This core debris may interact with the concrete containment floor, oxidizing metallic species in the debris.

Throughout these events, steam is generated in the RPV. In addition, when the core materials oxidize, hydrogen is generated. The steam and hydrogen are vented through the SRVs or through a leak in the RCP seals if leakage is assumed to occur. Steam flowing through the SRVs is vented into the suppression pool where it can be condensed. In the case of a RCP leak, steam and hydrogen are directly vented to the DW. In all cases, containment pressurizes over time due to the addition of steam and noncondensable gases.

As modeled during the scenario, operators either refrain from taking action to vent containment, or their actions are unsuccessful. The containment eventually fails, releasing radionuclides and hydrogen into the reactor building. Deflagrations can occur in the reactor building, and ultimately radionuclides can be released into the environment. The scenario was simulated for 32 h.

3.4.1.1 Parametric study cases

For the LTSBO scenario, simulation cases included variations in the following:

- Flooding of the DW head cavity region: not flooded, or flooded 2 or 8 hours after accident initiation
- DW discretization and heat transfer model: either the basic discretization that uses the parametric heat transfer model (Sections 3.3.3.1 and 3.3.2.1) or the refined discretization that uses the integrated physics heat transfer model (Sections 3.3.3.2 and 3.3.2.2)
- DW head leakage model: either the T&P limit model (Section 3.3.4.1) or the variable area model (Section 3.3.4.2)
- RCP leakage assumption: either modeled to occur (Section 3.3.5.2) or not.
- DW head heat transfer area: baseline area or 3× baseline area (Section 3.3.2.2)

The combination of cases considered is summarized in Section 3.4.3.

3.4.2 Extended Loss of AC Power Scenario

For the ELAP scenario, the reactor is assumed to successfully trip (reference time 0 h). All AC power, including off-site and onsite AC power (diesel generators), is assumed to be lost at 0 h. However, DC power is assumed to remain online either through recharging the station batteries or other means.

With DC power, the RCIC and HPCI systems can be used to inject cooling water into the primary system. As modeled, operators do not control the speed of the RCIC or HPCI systems. Thus, they turn full-on and off as necessitated by the water level. Also, as modeled, these systems are initially aligned to take suction from the condensate storage tank. Steam generated in the RPV is vented through the RCIC, HPCI, or the SRVs. As modeled, the operators will use an SRV to manually depressurize the RPV down to approximately 1.14 MPa (150 psig) if the suppression pool exceeds its heat capacity limit.

After depletion of the condensation storage tank, the RCIC and HPCI are realigned to take suction from the suppression pool. However, the suppression pool and containment increase in temperature and pressure over the course of the accident scenario. For the scenario modeled, the RCIC and HPCI are isolated approximately 11 hours into the accident due to net positive suction head limits. Supplemental injection into the feedwater line is assumed to commence 12 hours into the accident scenario. Table 7 provides the assumed total injection flow rate versus time. The water injection rate is sufficient to offset the decay heat and keep the core covered. Since sufficient cooling water is supplied to the RPV to offset the decay heat, the core remains covered, and the fuel does not degrade.

As modeled during the scenario, the operators either refrain from taking action to vent containment, or their actions are unsuccessful. Over time, the suppression pool temperature increases, and containment pressurizes. The scenario was simulated for 72 h.

Table 7. Supplemental injection timing and rate during ELAP

Time interval (h)	Injection rate	
	(lpm)	(gpm)
0–12	0.0	0
12–36	416.4	110
36–54	378.5	100
54–72	340.7	90

3.4.2.1 Parametric study cases

For the ELAP scenario, simulation cases included variations in the following:

- Flooding of the DW head cavity region: not flooded, or flooded 2 or 8 hours after accident initiation
- DW discretization and heat transfer model: either the basic discretization that uses the parametric heat transfer model (Sections 3.3.3.1 and 3.3.2.1) or the refined discretization that uses the integrated physics heat transfer model (Sections 3.3.3.2 and 3.3.2.2)
- DW head leakage model: either the T&P limit model (Section 3.3.4.1) or the variable area model (Section 3.3.4.2)
- DW head heat transfer area: baseline area or 3× baseline area (Section 3.3.2.2)

All cases assumed that no RCP seal leakage occurs. The combination of cases considered is summarized in Section 3.4.3.

3.4.3 Simulation Summary

The simulations analyzed in Section 4 are summarized in Table 8 and Table 9. Each scenario simulates a case with and without flooding of the DW head cavity. The effects of DW discretization modeling and associated modeling of DW head heat transfer, DW head flange seal leakage modeling, RCP leakage, and the timing of flooding are investigated. In total, 24 cases were simulated, providing for 9 comparisons between the DW head cooling mitigation action vs no mitigation action. In addition, two scenarios were modeled for which the heat transfer area of the DW head were enhanced, Table 9

Table 8. Summary of simulation cases

Scenario	DW discretization and heat transfer models	DW head flange seal leak model	RCP leakage	Flooding DW head timing (h)	Case
LTSBO	Basic disc. with parametric heat transfer model	T&P limit	No	None	1
				2	2
			Yes	None	3
				2	4
				8	19
		Variable area	No	None	5
				2	6
			Yes	None	7
				2	8
				8	20
	Refined disc. with integrated physics heat transfer model	Variable area	No	None	13
				2	14
			Yes	None	17
				2	18
				8	21
ELAP	Basic disc. with parametric heat transfer model	T&P limit	No	None	9
				2	10
				8	22
		Variable area	No	None	11
				2	12
				8	23
	Refined disc. with integrated physics heat transfer model	Variable area	No	None	15
				2	16
				8	24

Table 9. Summary of DW head heat transfer area variation cases

Scenario	DW discretization and heat transfer models	DW head flange seal leak model	RCP leakage	Flooding DW head timing (h)	DW head heat transfer area	Case
LTSBO	Refined disc. with integrated physics heat transfer model	Variable area	Yes	None	1×	17
				2	1×	18
				None	3×	25
				2	3×	26
ELAP	Refined disc. with integrated physics heat transfer model	Variable area	No	None	1×	15
				2	1×	16
				None	3×	27
				2	3×	28

4. INTEGRAL ANALYSIS SIMULATIONS RESULTS

Sections 4.1 and 4.2 present and discuss simulation results for the LTSBO and ELAP scenarios, respectively. This is followed by LTSBO and ELAP scenario simulations in which the effect of the head heat transfer area was is investigated (Section 4.3). Key results are discussed in Section 4.4. For each scenario, a general overview of the accident progression is provided, followed by the figure of merit results for each scenario.

4.1 LTSBO SCENARIO

4.1.1 Without RCP Leakage – Flooding at 2h

The results of the figures of merit for Cases 1, 2, 5, 6, 13, and 14 are summarized in Table 10 through Table 13. Red shading indicates a negative effect of the mitigation action while green shading indicates a positive effect. Plots of the DW pressure and gas concentrations are provided in Appendix A.

Without leakage through the RCP seals, the DW slowly pressurizes over the 0–12 h timeframe. During this time, concentration of nitrogen in the DW remains high, and the heat removal through the drywell head remains low at <200 kW. The steam being vented into the suppression pool through the SRVs and RCIC/HPCI systems increases the pool temperature. After being realigned to take suction from the suppression pool, the RCIC and HPCI systems are isolated at around the 12.5–13.0 h timeframe due to net positive suction head limits. Additional steam is vented to the suppression pool as the water in the RPV boils away and core degradation commences. The exothermic oxidation of core materials results in (1) additional energy being released into the wetwell through generation of steam and/or superheating of steam and (2) venting of hydrogen into the suppression pool. These factors result in faster pressurization and increased steam concentration in the DW. The generation of hydrogen and its migration to the DW causes a decrease in the efficacy of the DW head cooling mitigation action. For Cases 2 and 6—which use the basic containment discretization with the correlated head heat transfer model—heat transfer through the DW head region ceases at around 16 h. Heat transfer is modeled to cease when ≥10 kg of hydrogen is in the DW. Eventually the increased temperature and pressure in the PCV causes a failure either in the wetwell or the DW.

Table 10. LTSBO figure of merit results: basic discretization, T&P head leakage, no RCP pump leak

Figure of merit	Case 1: not flooded	Case 2: flooded	Difference
DW reaches 0.49 MPa (56 psig) [a]	1,022	986	-36
Containment failure [a]	1,464	1,434	-30
First deflagration in building [a]	1,464	1,434	-30
0.5 kg of noble gas release to environment [a]	1,464	1,434	-30

[a] = *minute*

Table 11. LTSBO figure of merit results: basic discretization, variable area head leakage, no RCP pump leak

Figure of merit	Case 5: not flooded	Case 6: flooded	Difference
DW reaches 0.49 MPa (56 psig) [a]	1,022	986	-36
Containment failure [a]	1,054	1,046	-9
First deflagration in building [a]	1,055	1,046	-10
0.5 kg of noble gas release to environment [a]	1,076	1,160	84

[a] = *minute*

Table 12. LTSBO figure of merit results: refined discretization, variable area head leakage, no RCP pump leak

Figure of merit	Case 13: not flooded	Case 14: flooded	Difference
DW reaches 0.49 MPa (56 psig) [a]	1,004	1,006	2
Containment failure [a]	1,047	1,071	24
First deflagration in building [a]	1,049	1,073	23
0.5 kg of noble gas release to environment [a]	1,066	1,182	116

[a] = minute

Table 13. Ratio of radionuclide releases

Figure of merit	Ratio of flooded vs not flooded		
	Cases 1 & 2	Cases 5 & 6	Cases 13 & 14
Class 2, 4, 16 (Cs, I, CsI . . .) to environment [a]	1.90	0.04	0.20
Class 3 (Sr, Ba . . .) to environment [a]	1.33	0.16	0.10

[a] = ratio of the fractions of inventory released by the end of simulation

The first containment failure mode predicted for Cases 1 and 2 is the rupture of the wetwell. (Note that Case 1 was near the failure point of the DW head flange seal.) With this failure mode, the potential scrubbing capability of the flooded DW head cavity is thwarted, so the mitigation action has little impact, and it is actually predicted to have a slightly detrimental effect on the predicted fission product releases. The heat transfer predicted for the mitigation action is less than 300 kW throughout the simulation. Interestingly, the hydrogen concentration in the DW is predicted to decrease at around the 26 h mark, and heat transfer through the DW head is predicted to temporarily resume.

The first containment failure mode predicted for Cases 5 and 6 are leakage through the DW head flange seal. The heat transfer through the DW head region is low at less than 300 kW throughout the simulation. The onset of leakage is predicted to occur at similar times, irrespective of the mitigation action. With the mitigation action, the onset of radionuclide releases to the environment is delayed 84 minutes, and substantially less Class 2, 4, 16, and 3 fission products are predicted to be released to the environment by the end of the simulation.

The first containment failure mode predicted for Cases 13 and 14 is leakage through the DW head flange seal. The heat transfer through the DW head region varies, with early spikes related to quenching of the drywell head structures, followed by a longer period of lower heat transfer (<300 kW). As containment pressurizes, heat transfer is predicted to increase up to 1.5 MW before the DW head is predicted to begin leaking. With the mitigation action, the onset of containment failure, defined as leakage through the DW flange seal, is delayed 24 minutes. After the drywell head begins leaking, the DW pressure stabilizes, the steam concentration generally increases, and the heat transfer remains at levels above 1 MW. With the mitigation action, the onset of radionuclide releases to the environment is delayed by 116 minutes, and substantially less Class 2, 4, 16 and 3 fission products are predicted to be released to the environment by the end of the simulation.

4.1.2 With RCP Leakage

The results of the figures of merit for Cases 3, 4, 7–9, and 17–21 are summarized in Table 14 through Table 18. Plots of the DW pressure and gas concentrations are provided in Appendix A.

With leakage through the RCP seals, the DW pressurizes faster over the 0–12 h timeframe. After onset of the RCP leakage (10 minutes after shutdown), the concentration of nitrogen in the DW rapidly decreases, while the steam concentration increases. For cases in which the DW head cavity is flooded beginning at 2 h (mitigation action), the steam in the DW is condensed, the pressure stabilizes, and the nitrogen concentration increases. For cases in which the DW head cavity is not flooded, the containment continues to pressurize, with the nitrogen concentration decreasing and the steam concentration increasing over time. Like the LTSBO without RCP leakage (Section 4.1.1), the steam being vented into the suppression pool through the SRVs and RCIC/HPCI systems increases the pool's temperature. After being realigned to take suction from the suppression pool, the RCIC and HPCI systems are isolated at around the 12.5–13.0 h timeframe due to net positive suction head limits. Additional steam is vented to the suppression pool as the water in the RPV boils away and core degradation commences. The exothermic oxidation of core materials results in (1) additional energy being released into the wetwell through generation of steam and/or superheating of steam and (2) venting of hydrogen into the suppression pool. These factors contribute to the pressurization and increased steam concentration in the DW. Generation of hydrogen and its migration to the DW causes a decrease in the efficacy of the DW head cooling mitigation action. For Cases 4, 8, 19 and 20, which utilize the basic containment discretization with the correlated head heat transfer model, heat transfer through the DW head region ceases at around 15.5 h (modeled to cease when ≥10 kg of hydrogen is in the DW). Eventually, the increased temperature and pressure in the PCV causes a failure either in the wetwell or the DW.

Table 14. LTSBO figure of merit results: basic discretization, T&P head leakage, with RCP pump leak

Figure of merit	Case 3: not flooded	Case 4: flooded 2h	Case 19: flooded 8h	Difference Cases 3 & 4	Difference Cases 3–19
DW reaches 0.49 MPa (56 psig) [a]	916	941	941	25	25
Containment failure [a]	1,186	1,299	1,270	112	84
First deflagration in building [a]	1,187	1,299	1,270	112	83
0.5 kg of noble gas release to environment [a]	1,188	1,299	1,270	111	82

[a] = minute

Table 15. LTSBO figure of merit results: basic discretization, variable area head leakage, with RCP pump leak

Figure of merit	Case 7: not flooded	Case 8: flooded 2h	Case 20: flooded 8h	Difference Cases 7–8	Difference Cases 7–20
DW reaches 0.49 MPa (56 psig) [a]	916	941	938	25	22
Containment failure [a]	937	983	978	46	41
First deflagration in building [a]	1,068	983	978	-85	-90
0.5 kg of noble gas release to environment [a]	980	1,029	1,017	49	37

[a] = minute

Table 16. LTSBO figure of merit results: refined discretization, variable area head leakage, with RCP pump leak

Figure of merit	Case 17: not flooded	Case 18: flooded 2h	Case 21: flooded 8h	Difference Case 17 - 18	Difference Case 17 - 21
DW reaches 0.49 MPa (56 psig) [a]	931	947	944	16	13
Containment failure [a]	951	989	986	39	35
First deflagration in building [a]	1,038	990	986	-48	-52
0.5 kg of noble gas release to environment [a]	980	1,031	1,064	52	84

[a] = minute

Table 17. Ratio of radionuclide releases, flooding initiated at 2 hours

Figure of merit	Ratio of flooded vs. not flooded		
	Cases 3 & 4	Cases 7 & 8	Cases 17 & 18
Class 2, 4, 16 (Cs, I, CsI . . .) to environment [a]	0.15	0.13	0.86
Class 3 (Sr, Ba . . .) to environment [a]	0.02	0.004	2.44

[a] = *ratio of the fractions of inventory released by the end of simulation*

Table 18. Ratio of radionuclide releases, flooding initiated at 8 hours

Figure of merit	Ratio of flooded vs. not flooded		
	Cases 3 & 19	Cases 7 & 20	Cases 17 & 21
Class 2, 4, 16 (Cs, I, CsI . . .) to environment [a]	0.40	0.10	0.08
Class 3 (Sr, Ba . . .) to environment [a]	0.21	0.002	0.01

[a] = *ratio of the fractions of inventory released by the end of simulation*

The first containment failure mode predicted for Case 3 is DW head leakage, while rupture of the wetwell is predicted for Cases 4 and 19. The heat transfer through the DW head region is low at less than 350 kW throughout the simulation; however, it is higher than the comparable Case 2 without RCP leakage. The onset of PCV failure is delayed by the mitigation action by 112 minutes for flooding initiated at 2 hours and 84 minutes when flooding is initiated at 8 hours. With rupture of the wetwell, the potential scrubbing capability of the flooded DW head cavity is thwarted for Cases 4 and 19. However, fission product release to the environment is delayed by 111 minutes for Case 4 and 84 minutes for Case 19. Substantially less Class 2, 4, and 16 and Class 3 fission products are predicted to be released to the environment by the end of the simulations with the mitigation action.

The first containment failure mode predicted for Cases 7, 8, and 20 is leakage through the DW head flange seal. The heat transfer through the DW head region is low at less than 350 kW throughout the simulation. The onset of PCV failure is delayed by the mitigation action by 46 minutes when flooding is initiated at 2 hours, and it is delayed by and 41 minutes when flooding is initiated at 8 hours. The onset of radionuclide releases to the environment is delayed 49 minutes when flooding is initiated at 2 hours, and it is delayed by 37 minutes when flooding is initiated at 8 hours. Substantially less Class 2, 4, and 16 and Class 3 fission products are predicted to be released to the environment by the end of the simulation with the mitigation action.

The first containment failure mode predicted for Cases 17, 18 and 21 is leakage through the DW head flange seal. The heat transfer through the DW head region varies, with early spikes related to quenching the drywell head structures, followed by a longer period of moderate heat transfer (<2 MW). As containment pressurizes, heat transfer is predicted to increase up to 2 MW before the DW head is predicted to begin leaking at 16.5 hours. The onset of containment failure, which is defined as leakage through the DW flange seal, is delayed 39 minutes when flooding is initiated at 2 hours and 35 minutes when flooding is initiated at 8 hours. After the drywell head begins leaking, the DW pressure stabilizes, the steam concentration generally increases, and the heat transfer remains at levels above 1 MW. The onset of radionuclide releases to the environment is delayed 52 minutes when flooding is initiated at 2 hours and 84 minutes when flooding is initiated at 8 hours. Substantially less Class 2, 4, and 16 fission products are predicted to be released to the environment by the end of the simulation for cases with the mitigation action. Interestingly, the amount of Class 3 fission products released to the environment by the end of Case 18 simulation is predicted to be higher.

The different releases are due to the later predicted containment failure modes. The second containment failure mode, wetwell rupture, is predicted to occur for Case 17 at 30.3 h into the accident scenario, whereas the DW liner melt-through is eventually predicted for Case 18. For Cases 17 and 18, releases through the RCP seals would initially bypass the suppression pool (i.e., scrubbing by the suppression pool) and would be released out of the DW head flange. However, after failure of the wetwell in Case 17, the DW gases would pass through the suppression pool before being released out of the wetwell. In contrast, with liner melt-through occurring in Case 18, the radionuclides could be released through this failure point without being scrubbed by the suppression pool.

4.2 ELAP SCENARIO

The results of the figures of merit for Cases 9–12, 15, 16, and 22–24 are summarized in Table 19 through Table 21. Plots of the DW pressure and gas concentrations are provided in Appendix A.

Without leakage through the RCP seals, the DW slowly pressurizes over the course of the accident. The concentration of nitrogen in the DW steadily decreases, while the steam concentration increases. As containment pressurizes and the steam concentration increases, the heat removal through the drywell head for the cases employing the mitigation action steadily increases, reaching values greater than 2 MW. For most cases, the DW head flange seal is predicted to eventually fail. Initially, the RCIC and/or HPCI systems provide makeup water to the RPV. In the longer term, the supplemental water injection keeps the core covered. As the core remains covered, the fuel remains relatively cool, hydrogen is not generated, and fission products are not released.

Table 19. ELAP figure of merit results: basic discretization, T&P limit head leakage, no RCP pump leak

Figure of merit	Case 9: not flooded	Case 10: flooded 2h	Case 22: flooded 8h	Difference Cases 9–10	Difference Cases 9–22
DW reaches 0.49 MPa (56 psig) [a]	1,520	1,631	1,647	111	127
Containment failure [a]	2,652	NA	NA	>1,668	>1,668

[a] = minute

Table 20. ELAP figure of merit results: basic discretization, variable area head leakage, no RCP pump leak

Figure of merit	Case 11: not flooded	Case 12: flooded 2h	Case 23: flooded 8h	Difference Cases 11–12	Difference Cases 11–23
DW reaches 0.49 MPa (56 psig) [a]	1,520	1,631	1,647	111	127
Containment failure [a]	1,812	2,072	2,071	260	259

[a] = minute

Table 21. ELAP figure of merit results: refined discretization, variable area head leakage, no RCP pump leak

Figure of merit	Case 15: not flooded	Case 16: flooded 2h	Case 24: flooded 8h	Difference Cases 15–16	Difference Cases 15–24
DW reaches 0.49 MPa (56 psig) [a]	1,509	1,641	1,650	132	141
Containment failure [a]	1,795	2,018	2,022	223	227

[a] = minute

The first containment failure mode predicted for Case 9 is DW head leakage, while no failure is predicted for Cases 10 & 22. The heat transfer through the DW head region steadily increases throughout the

simulation, reaching a value of 2.5 MW by the end of the simulation. As the PCV did not fail for Cases 10 or 22 within the 72 h of simulated time, the onset of PCV failure is delayed by the mitigation action by at least 1,668 minutes (27.8 h).

The first containment failure mode predicted for Cases 11, 12 and 23 is leakage through the DW head flange seal. The heat transfer through the DW head region steadily increases throughout the simulation, reaching a value of 3 MW by the end of the simulation. The onset of PCV failure is delayed by the mitigation action by 259-260 minutes (4.3 h).

The first containment failure mode predicted for Cases 15, 16 and 24 is leakage through the DW head flange seal. The heat transfer through the DW head region steadily increases throughout the simulation, reaching a high value of 8.6 MW by the end of the simulation. The onset of PCV failure is delayed by the mitigation action by 223-227 minutes (3.7 h).

4.3 IMPACT OF DW HEAD SURFACE AREA

The results of the figures of merit for the LTSBO Cases 17, 18, 25 and 26 are summarized in Table 22. Plots of the DW pressure, gas concentrations and heat removal are provided in Appendix A.

Table 22. LTSBO figure of merit results: refined discretization, variable area head leakage, with RCP pump leak, variation in DW head area

Figure of merit	Case 17: not flooded 1× area	Case 25: not flooded 3× area	Case 18: flooded 1× area	Case 26: flooded 3× area
DW reaches 0.49 MPa (56 psig) [a]	931	927	947	942
Containment failure [a]	951	959	989	1,000
First deflagration in building [a]	1,038	1,057	990	1,001
0.5 kg of noble gas release to environment [a]	980	982	1,031	1,112

[a] = *minute*

For Cases 17 and 25, in which the mitigation action was not implemented, the increase in the DW head surface area had a minor impact on the timing of the accident progression. The largest impact was in delaying the first deflagration in the building by 19 minutes. Similarly, for cases in which the mitigation action was implemented, there were only minor differences in the accident progression timing. The largest impact was in delaying the onset of noble gas release to the environment by an additional 81 minutes.

The results of the figures of merit for the ELAP Cases 15, 16, 27, and 28 are summarized in Table 23. Plots of the DW pressure, gas concentrations and heat removal are provided in Appendix A.

Table 23. ELAP figure of merit results: refined discretization, variable area head leakage, no RCP pump leak, variation in DW head area

Figure of merit	Case 15: not flooded 1× area	Case 27: not flooded 3× area	Case 16: flooded 1× area	Case 28: flooded 3× area
DW reaches 0.49 MPa (56 psig) [a]	1,509	1539	1,641	1,702
Containment failure [a]	1,795	1791	2,018	2,256

[a] = *minute*

The containment for Cases 15, 16, 27, and 28—which all used the variable area DW head leakage model—was predicted to eventually fail at the DW head flange. For Cases 15 and 27, in which the

mitigation action was not implemented, the increase in the DW head surface area again had a minor impact on the timing of the accident progression. The largest impact was in delaying containment reaching 56 psig by 30 minutes.

For the cases in which the mitigation action was implemented, increasing the DW head surface area had a larger impact. The time for the DW to reach 56 psig was extended an additional 61 minutes (from 2.2 to 3.2 hours). The timing of first containment failure was also further delayed by an additional 238 minutes (from 3.7 to 7.7 hours). Initially, Case 28, with the increase DW head heat transfer area, was predicted to have higher heat transfer through the head, which slowed the DW pressurization more so than in Case 16. After failure of the DW head flange, Cases 16 and 28 were predicted to have similar heat transfer rates of approximately 8.8 MW.

4.4 SUMMARY AND DISCUSSION OF RESULTS

4.4.1 Timing of Initial PCV Failure

The differences in the initial PCV failure timings between the cases with and without mitigation action are summarized in Table 24 through Table 27. For the majority of cases, the mitigation action delays the initial PCV failure.

For the LTSBO simulations without direct leakage from the RPV into the DW, the delay in initial PCV failure varies from -0.5 h to +0.4 h. Before the PCV is predicted to fail, the relatively low DW pressure, coupled with the low DW steam concentration, yields a relatively low potential for heat removal (<300 kW). The onset of hydrogen generation at around 16 h into the accident scenario causes the DW to pressurize while at the same time limiting the potential heat transfer through the DW head region.

For the LTSBO simulations with direct leakage from the RPV into the DW, the delay in initial PCV failure varies from 0.58–1.9 h, depending on the DW head leakage model, the DW discretization and accompanying heat transfer model of the DW head, and the timing of the mitigation initiation. The RPV leak provides steam directly into the DW, increasing both the DW pressure and steam concentration. Both of these factors increase the potential heat removal through the DW head, making the mitigation action more impactful.

The mitigation action had the strongest effect on delaying the PCV failure for the ELAP scenarios. Even without any direct leakage from the RPV into the DW, the delay in initial PCV failure varies from 3.7 h to over 27 h.

Using the DW head leakage model had a strong effect on the predicted delay in PCV failure. The T&P limit model predicted the onset of DW head leakage at pressures higher than that by the variable area model. The DW discretization and associated DW head heat transfer model had a secondary impact on the predicted delay in PCV failure.

Table 24. Additional time (min) between initial PCV failures due to mitigation action: LTSBO scenario – flooding at 2h

DW discretization model	DW head leak model	RCP leak	
		No	Yes
Basic	T&P limit	-30[a]	112
	Variable area	-9	46
Refined	Variable area	24	39

[a] *minutes*

Table 25. Additional time (min) between initial PCV failures due to mitigation action: LTSBO scenario – flooding at 8h

DW discretization model	DW head leak model	RCP leak	
		No	Yes
Basic	T&P limit	NS	84[a]
	Variable area	NS	41
Refined	Variable area	NS	35

[a] minutes NS = not simulated

Table 26. Additional time (min) between initial PCV failures due to mitigation action: ELAP scenario – flooding at 2h

DW discretization model	DW head leak model	RCP leak	
		No	Yes
Basic	T&P limit	>1,668[a,b]	NS
	Variable area	260	NS
Refined	Variable area	223	NS

[a] = minutes NS = not simulated
[b] = containment did not fail within 72 h of simulated time

Table 27. Additional time (min) between initial PCV failures due to mitigation action: ELAP scenario – flooding at 8h

DW discretization model	DW head leak model	RCP leak	
		No	Yes
Basic	T&P limit	>1,668[a,b]	NS
	Variable area	259	NS
Refined	Variable area	227	NS

[a] = minutes NS = not simulated
[b] = containment did not fail within 72 h of simulated time

4.4.2 PCV Failure Locations and Modes

The predicted location for the initial PCV failure is summarized in Table 28. In the majority of cases, the DW head flange seal is predicted to fail first. Rupture of the wetwell is predicted to occur first for cases in which the T&P DW head leakage model is used, except in Case 3. This model allows for higher DW pressures before head seal leakage than the variable area model. Effectively, there is a competition between the DW head seal failure and the wetwell failure, both of which are modeled to occur at 1,067 kPa (140 psig) at low temperatures.

The subsequent second and third PCV failure locations and modes are summarized in Table 29. For the LSTBO scenario, in which core melt is released from the RPV, melt-through of the DW liner and/or rupture due to high temperatures is predicted to occur in some cases. In general, the mitigation action limits the occurrence of these secondary and tertiary containment failure modes compared to the cases without the mitigation action. The mitigation action helps reduce DW temperatures, resulting in increased condensed water on the DW floor, as shown in Table 30. The addition water on the DW floor would enhance melt coolability and decrease the potential of the liner melting through. As noted in Section 3.3.8, limitations in the core-concrete interaction modeling of MELCOR 1.8.6 will likely affect the

predicted efficacy of this additional cooling water on debris coolability: the effect of additional water on the DW floor water may be underestimated.

For the ELAP scenario, a secondary failure mode is not predicted for the majority of the cases. In this scenario, melt is not released from the RPV, and DW temperatures remain relatively low.

Table 28. Initial PCV failure locations

Scenario	DW discretization model	DW head flange seal leak model	RCP leakage	First PCV failure location		
				Without flooding	With flooding at 2 hours	With flooding at 8 hours
LTSBO	Basic	T&P limit	No	WW rupture	WW rupture	NS
			Yes	DW head flange	WW rupture	WW rupture
		Variable area	No	DW head flange	DW head flange	NS
			Yes	DW head flange	DW head flange	DW head flange
	Refined	Variable area	No	DW head flange	DW head flange	NS
			Yes	DW head flange	DW head flange	DW head flange
ELAP	Basic	T&P limit	No	WW rupture	NA	NA
		Variable area	No	DW head flange	DW head flange	DW head flange
	Refined	Variable area	No	DW head flange	DW head flange	DW head flange

NA = not applicable, PCV did not fail within 72 h of simulated time; NS = not simulated

Table 29. Second and third PCV failure locations

Scenario	DW discretization model	DW head flange seal leak model	RCP leakage	2nd and 3rd PCV failure location		
				Without flooding	With flooding at 2 hours	With flooding at 8 hours
LTSBO	Basic	T&P limit	No	Liner melt through DW liner rupture	Liner melt through DW liner rupture	NS
			Yes	Liner melt through	NA	Liner melt-through DW liner rupture
		Variable area	No	Liner melt through	NA	NS
			Yes	DW liner rupture	Liner melt through	NA
	Refined	Variable area	No	Liner melt through	NA	NS
			Yes	DW liner rupture	NA	NA
ELAP	Basic	T&P limit	No	WW rupture	NA	NA
		Variable area	No	NA	NA	NA
	Refined	Variable area	No	NA	NA	NA

NA = not applicable, did not occur before end of simulated time; NS = not simulated

Table 30. Additional water on DW floor (kg) due to mitigation action: LTSBO scenario

DW discretization model	DW head leak model	RCP leak	
		No	Yes
Basic	T&P limit	3,883[a] (62%)	12,891[a] (13%)
	Variable area	4,461 (82%)	12,363 (12%)
Refined	Variable area	6,726 (92%)	14,404 (15%)

[a] = kg

4.4.3 Potential Impact on Off-Site Releases

For the LTSBO scenario in which there is fuel damage and the release of fission products, the mitigation action delays the onset of fission product releases to the environment in the majority of cases. Except for

Cases 1 and 2, the mitigation action delays release by 0.6–1.9 h. Slightly earlier releases at 0.5 h are predicted for Case 2 in comparison to Case 1.

Table 31. Additional time (min) between onset of releases to the environment due to mitigation action: LTSBO scenario

DW discretization model	DW head leak model	No RCP leak	With RCP leak	
		Flooding at 2 hours	Flooding at 2 hours	Flooding at 8 hours
Basic	T&P limit	-30[a]	111	82
	Variable area	84	49	37
Refined	Variable area	116	52	84

[a] minutes

In addition to delaying the onset of release, the amount of Class 2, 4, 16, and 3 fission products released to the environment by the end of the simulations are reduced for the majority of the cases. For Cases 1 and 2, in which the initial containment failure mode is the rupture of the wetwell, there is a modest increase (33–90%) in releases with the mitigation action. In addition, in Cases 17 and 18, there is a 144% increase in the release of Class 3 fission products with the mitigation action stemming from the prediction of eventual liner melt through. However, in the other cases, the amount of Class 2, 4, and 16 fission products released by the end of the simulation is reduced by 14–92% and for Class 3 it is reduced by 79–99.8%.

As noted in Section 2.5, fission product scrubbing relies on an array of physics captured in MELCOR via a range of models and user options. The efficacy of water in the DW head cavity region in scrubbing of fission products requires more rigorous investigation. However, the results are as anticipated: if there is leakage through the DW head flange seal, water in the cavity will likely reduce the amount of fission products released to the environment.

Table 32. Ratios of releases of Class 2, 4, 16 (Cs, I, CsI, etc.) mitigated vs unmitigated action: LTSBO scenario

DW discretization model	DW head leak model	No RCP leak	With RCP leak	
		Flooding at 2 hours	Flooding at 2 hours	Flooding at 8 hours
Basic	T&P limit	1.90	0.15	0.40
	Variable area	0.04	0.13	0.10
Refined	Variable area	0.20	0.86	0.08

[a] = ratio of mitigated vs unmitigated values

Table 33. Ratios of releases of Class 3 (Sr, Ba, etc.) mitigated vs unmitigated action: LTSBO scenario

DW discretization model	DW head leak model	No RCP leak	With RCP leak	
		Flooding at 2 hours	Flooding at 2 hours	Flooding at 8 hours
Basic	T&P limit	1.33	0.02	0.21
	Variable area	0.16	0.004	0.002
Refined	Variable area	0.10	2.44	0.01

[a] ratio of mitigated vs unmitigated values

5. SUMMARY

An accident mitigation measure was proposed that is applicable to BWRs with Mark I and II containments. The mitigation measure is to externally flood the drywell head cavity during an accident. A scoping assessment was performed to analyze the potential effects of this accident mitigation measure.

The DW head cavity is located below the refueling floor. Gaps between the shield plugs that are located on the refueling floor above the cavity could facilitate flooding the cavity below. Depending on the accident scenario, the refueling floor may be accessible, as it is outside primary containment. Initially flooding the cavity may require a low-head high-capacity pump (500+ gpm), but to offset inventory losses over the long term, small capacity pumps could be used (<50 gpm). These are reasonably sized pumps and are likely available onsite, or some may be brought in from off-site.

For the assumed geometry, a surface area of 170 m^2 is available at the top of the DW for heat removal. Based on the available surface area, heat transfer analyses suggested that heat removal rates of up to several MW could be achieved. However, the pre-existing nitrogen in the PCV lowers the partial pressure of the steam in the DW and decreases the potential heat transfer. At DW temperatures below approximately 100 °C—low steam partial pressures—heat removal is limited by single phase convection on the external surface. At higher DW temperatures—higher steam partial pressures—boiling on the external surface of the DW head can commence, and heat transfer increases greatly. Hydrogen, which can be generated during oxidation of core materials, has a detrimental effect on the potential heat transfer.

Using the MELCOR code, integral simulations were conducted for LTSBO and ELAP accident scenarios, in which the mitigation action was either employed or not employed. In the scenarios, it was assumed that the operator did not vent the PCV. Simulations included variations in the DW head flange seal failure model, containment discretization and associated head heat transfer model, whether direct RPV-to-DW leakage was assumed, the initiation timing of the mitigation action, and the DW head heat transfer area. The simulation results were assessed for figures of merit related to timing of the accident scenario (pressurization, initial PCV failure, deflagrations, and fission product release) and reduction in offsite releases of fission products.

For the LTSBO scenario, the assumption as to whether direct RPV-to-DW leakage occurs influenced the efficacy of the mitigation action. For cases in which there was no RCP leakage, the mitigation action was determined to have limited effect on the timing of containment failure (delays of -0.5 to 0.4 h). For cases in which RCP leakage was assumed, the mitigation action had a larger effect and delayed PCV failure by 0.58–1.9 h. For the majority of cases, the mitigation action decreased off-site releases and reduced the occurrence of additional PCV failures later in the accident progression. In all cases, the mitigation action resulted in additional water on the DW floor before RPV failure. In general, the figures of merit were largely insensitive to the timing of initiating the accident mitigation measure (i.e., 2 h vs 8 h). For the scenario analyzed, increasing the DW head heat transfer surface area had a minor impact on the figures of merit.

For the ELAP scenario, the mitigation action had a more pronounced effect on delaying PCV failure. For cases using the variable area DW head flange failure model, the mitigation action delayed containment failure by 3.7–4.3 h. For the case using the T&P limit DW head flange failure model, the mitigation action prevented PCV failure throughout 72 h of simulated time (delayed failure more than 27.8 h). As no fission products are released in the ELAP scenario, related figures of merit were not assessed. As with the LTSBO scenario, the timing of initiating the accident mitigation measure generally had a minor

impact on the figures of merit. For the scenario analyzed, increasing the DW head heat transfer surface area delayed the first containment failure by an additional 4 hours (i.e. from 3.7 to 7.7 hours).

This scoping assessment only considered selected effects and accident scenarios. Further review, refinement, and validation of the models used for DW head seal failure, DW discretization, and fission product scrubbing would provide confidence in the assessment of the mitigation action efficacy. Considering a broader spectrum of accident scenarios including variations in event timing and other mitigation actions would result in a more comprehensive assessment of the proposed mitigation action. Considerations that were not investigated include cost-benefit analyses, plant-specific differences from that assumed in this analysis, other accident scenarios, human factors, seismic considerations, the potential impact on other accident mitigation actions, etc. These are areas for additional work if assessment of this accident mitigation measure is pursued further.

Notwithstanding future work, the current scoping assessment suggests that externally flooding the DW head cavity in BWRs with Mark I or II containments during beyond-design-basis accidents may have beneficial effects on the accident progression with respect to decreasing PCV pressure, delaying PCV failure and fission product releases, and scrubbing fission product releases.

6. REFERENCES

1. K. R. Robb, *External Cooling of the BWR Mark I and II Drywell Head as a Potential Accident Mitigation Measure–Scoping Assessment*, ORNL/TM-2017/457, Oak Ridge National Lab. (ORNL), Oak Ridge, TN (United States), 2017.
2. V. N. Shah, S. K. Smith, U. P. Sinha, *Insights for Aging Management of Light Water Reactor Components Vol. 5*, NUREG/CR-5314, EGG-2562, 1994.
3. S. R. Greene, *Realistic Simulation of Severe Accidents in BWRs – Computer Modeling Requirements*, NUREG/CR-2940, ORNL/TM-8517, 1984.
4. Nuclear Emergency Response Headquarters, Government of Japan, *Report of Japanese Government to the IAEA Ministerial Conference on Nuclear Safety — The Accident at TEPCO's Fukushima Nuclear Power Stations*, June 2011.
5. TEPCO Holdings Inc., *Parameters related to the plants at Fukushima Daiichi Nuclear Power Station*, http://www.tepco.co.jp/en/nu/fukushima-np/f1/pla/index-e.html, accessed August 24, 2017.
6. *Progress of Dismantling Work of the Building Cover of Fukushima Daiichi Nuclear Power Station Unit 1*, Document 2 A-1 (1), Presentation by TEPCO Holdings Company, November 21, 2016. http://www.tepco.co.jp/nu/fukushima-np/roadmap/images1/images2/l161121_10-j.pdf, (in Japanese) accessed July 2017.
7. TEPCO Holdings Inc., http://www.tepco.co.jp/nu/fukushima-np/roadmap/2017/images1/d170330_07-j.pdf, (in Japanese) accessed July 2017.
8. TEPCO Holdings *Air dose rates in the buildings*, http://www.tepco.co.jp/en/nu/fukushima-np/f1/surveymap/images/f1-sv3-20130322-e.pdf, accessed August 2017.
9. TEPCO Holdings Inc., *Result of temperature measurement by infrared camera from right above the reactor*, uploaded Oct 15,2011, pictured on Oct 13, 2011. http://photo.tepco.co.jp/en/date/2011/201110-e/111015-03e.html
10. R. O. Gauntt et al., *Fukushima Daiichi Accident Study (Status as of April 2012)*, SAND2012-6173, June 2012.
11. T. Sevón, "MELCOR model of Fukushima Daiichi Unit 1 accident," Annals of Nuc. E., **85,** 1-11 (2015).
12. D. Luxat, J. Gabor, R. Yang, F. Rahn, et al., *Fukushima Technical Evaluation Phase 1—MAAP5 Analysis*, EPRI, 1025750, Palo Alto, CA, 2013.
13. D. Luxat, R. Wachowiak, et al., *Technical Evaluation of Fukushima Accidents: Phase 2*, EPRI, 3002005301, Palo Alto, CA, 2015.
14. Nuclear Energy Institute, *Diverse and Flexible Coping Strategies (FLEX) Implementation Guide*, NEI 12-06 Rev. B1, May 2012.
15. I. Huhtiniemi and M. Corradini, "Condensation in the presence of noncondensable gases," *Nuc. Eng. Des.*, **141**, p 429, 1993.
16. Sandia National Laboratories, *MELCOR Computer Code Manuals*, Version 1.8.6, NUREG/CR-6119, Rev. 3, September 2005.
17. L. E. Herranz, M. H. Anderson, and M. L. Corradini, "A diffusion layer model for steam condensation within the AP600 containment," *Nuc. Eng. and Des.*, **183**, 133–150 (1998).
18. P. F. Peterson, "Theoretical basis for the Uchida correlation for condensation in reactor containments," *Nuc. Eng. and Des*., **162**, 301–306 (1996).
19. P. C. Owczarski and K. W. Burk, *SPARC-90: A Code for calculating fission product capture in suppression pools*, NUREG/CR-5765, Oct. 1991.
20. K. R. Robb, M. Howell, and L. J. Ott, *Parametric and experimentally informed BWR Severe Accident Analysis Utilizing FeCrAl - M3FT-17OR020205041*," ORNL/SPR-2017/373, August 2017.
21. K. R. Robb, *Updated Peach Bottom Model for MELCOR 1.8.6: Description and Comparisons*, ORNL/TM-2014/207, September 2014.

22. US Nuclear Regulatory Commission, *State-of-the-Art Reactor Consequence Analyses Project; Volume 1: Peach Bottom Integrated Analysis*, NUREG/CR-7110, Vol. 1, January 2012.
23. T. L. George, M. Marshall, O. E. Ozdemir, J. Zankowski, M. S. Lanza, S. W. Claybrook, and R. Wachowiak, *Fukushima Technical Evaluation, Phase 2—Revised GOTHIC Analysis*, EPRI 3002005295, Palo Alto, CA, 2015.
24. P. Mattie, et al., *State-of-the-Art Reactor Consequence Analyses Project - Uncertainty Analysis of the Unmitigated Long-Term Station Blackout of the Peach Bottom Atomic Power Station*, NUREG/CR-7155, SAND2012-10702P, May 2016.
25. Regulatory Issue Summary 2000-02, *Closure of Generic Safety Issue 23, Reactor Coolant Pump Seal Failure*, US Nuclear Regulatory Commission, February 15, 2000. (ML003680402)
26. C. J. Ruger and J. C. Higgins, *Reactor Coolant Pump Seal Issues and Their Applicability to New Reactor Designs*, BNL-NUREG-49115, Brookhaven National Laboratory, 1993.
27. T. Sevón, "MELCOR model of Fukushima Daiichi Unit 3 accident," *Nuc. Eng. and Des.*, **284,** 80–90 (2015).
28. D. Cook, *Pressure Suppression Pool Thermal Mixing*, NUREG/CR-3471, ORNL/TM-8906, 1984.
29. L. Herranz et al., "Influence of the wet-well nodalization of a BWR3 Mark I on the containment thermal-hydraulic response during an SBO," *Nuc. Eng. and Des.*, 295, pp 138–147, Dec. 2015.
30. K. R. Robb, M. T. Farmer, and M. W. Francis, *Ex-Vessel Core Melt Modeling Comparison between MELTSPREAD-CORQUENCH and MELCOR 2.1*, ORNL/TM-2014/1, March 2014.
31. US Nuclear Regulatory Commission, *Severe accident risks: an assessment for five US nuclear power plants*, NUREG-1150, US Nuclear Regulatory Commission, Washington, DC, 1990.

APPENDIX A: SIMULATION RESULT FIGURES

LSTBO scenario

Basic discretization, T&P limit DW failure, no RCP leakage

Basic discretization, variable area DW failure, no RCP leakage

Refined discretization, variable area DW failure, no RCP leakage

Basic discretization, T&P limit DW failure, with RCP leakage

Basic discretization, variable area DW failure, with RCP leakage

Refined discretization, variable area DW failure, with RCP leakage

Impact of DW head eat transfer area, refined discretization, variable area DW failure, with RCP leakage

ELAP scenario

Basic discretization, T&P limit DW failure, no RCP leakage

Basic discretization, variable area DW failure, no RCP leakage

Refined discretization, variable area DW failure, no RCP leakage

Impact of DW head eat transfer area, refined discretization, variable area DW failure, no RCP leakage

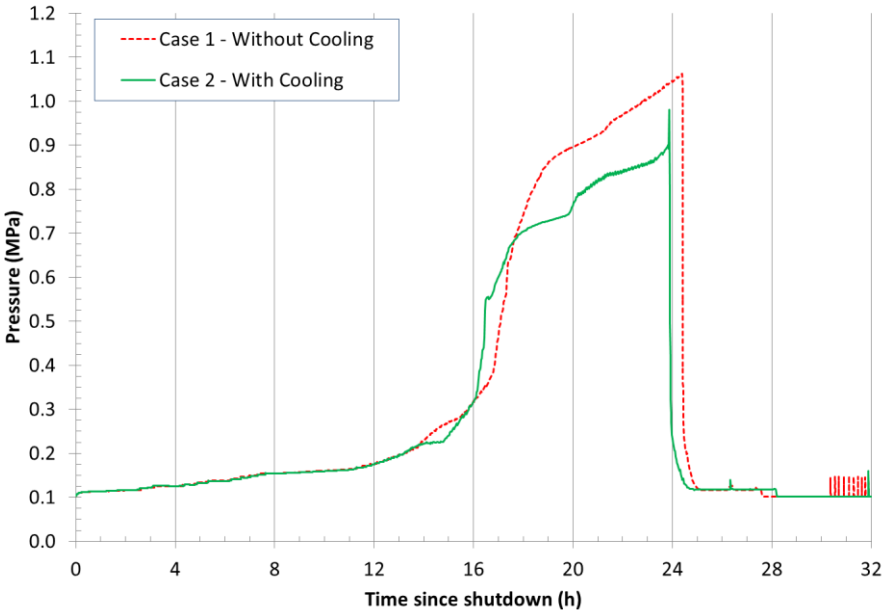

Figure A-1. LTSBO Cases 1 & 2: DW pressure.

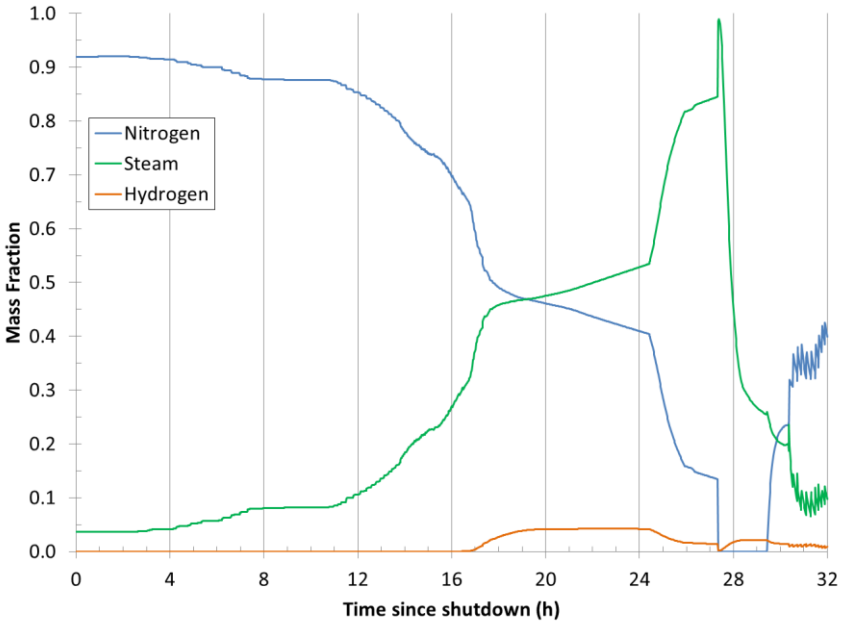

Figure A-2. LTSBO Case 1: DW gas concentrations.

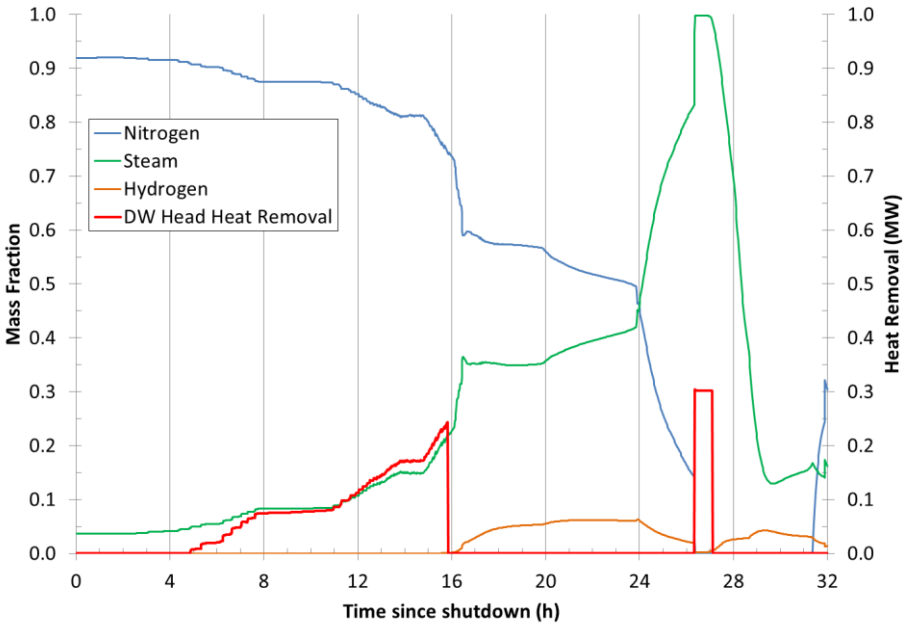

Figure A-3. LTSBO Case 2: DW gas concentrations and heat removal.

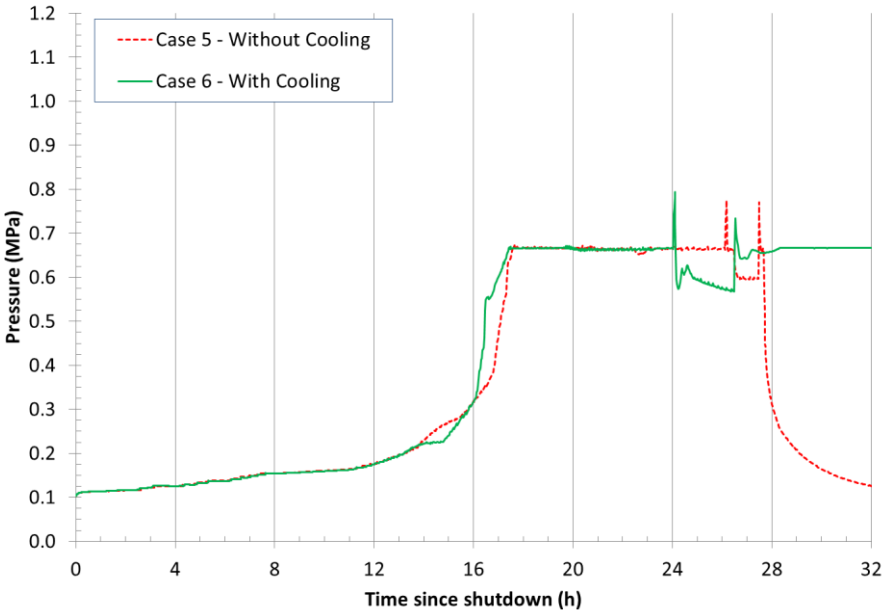

Figure A-4. LTSBO Cases 5 & 6: DW pressure.

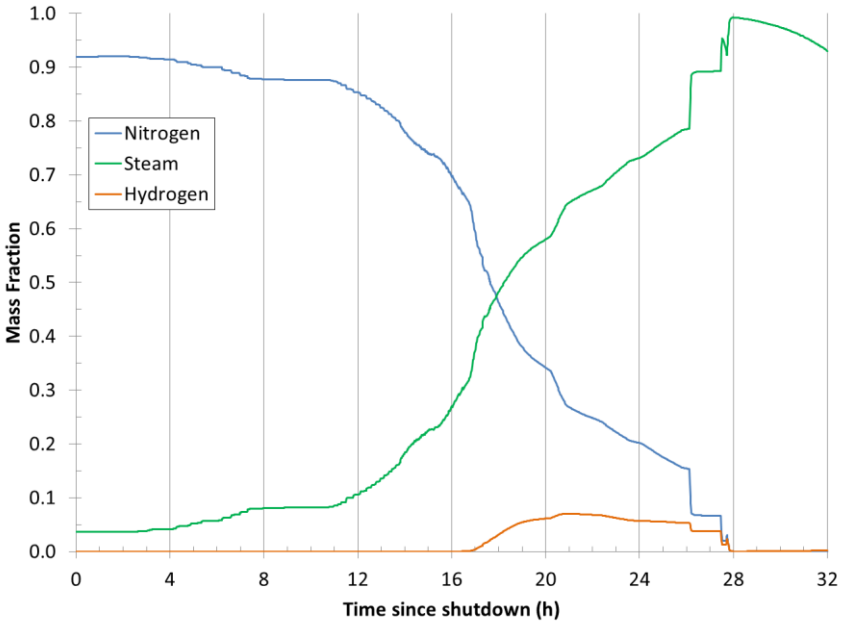

Figure A-5. LTSBO Case 5: DW gas concentrations.

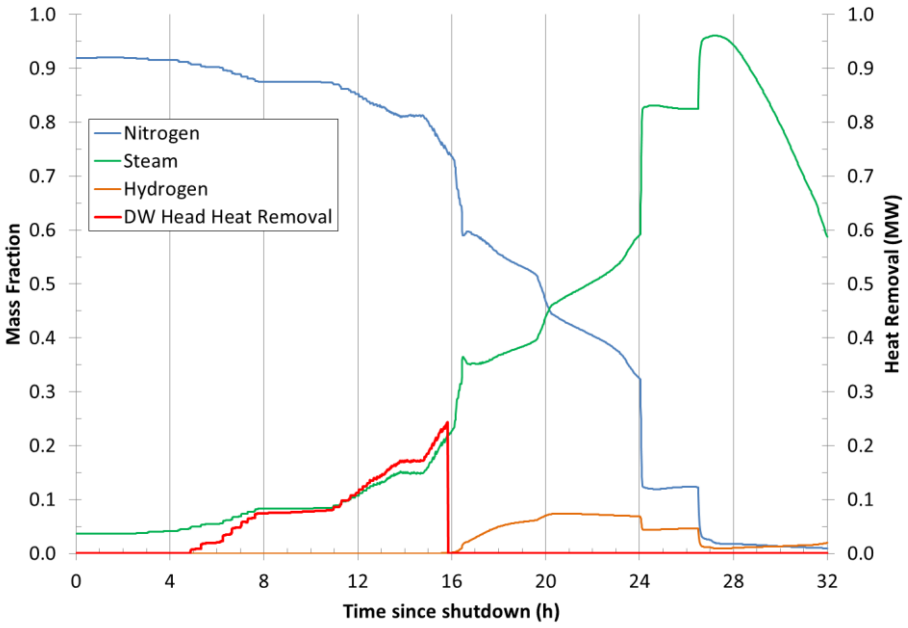

Figure A-6. LTSBO Case 6: DW gas concentrations and heat removal.

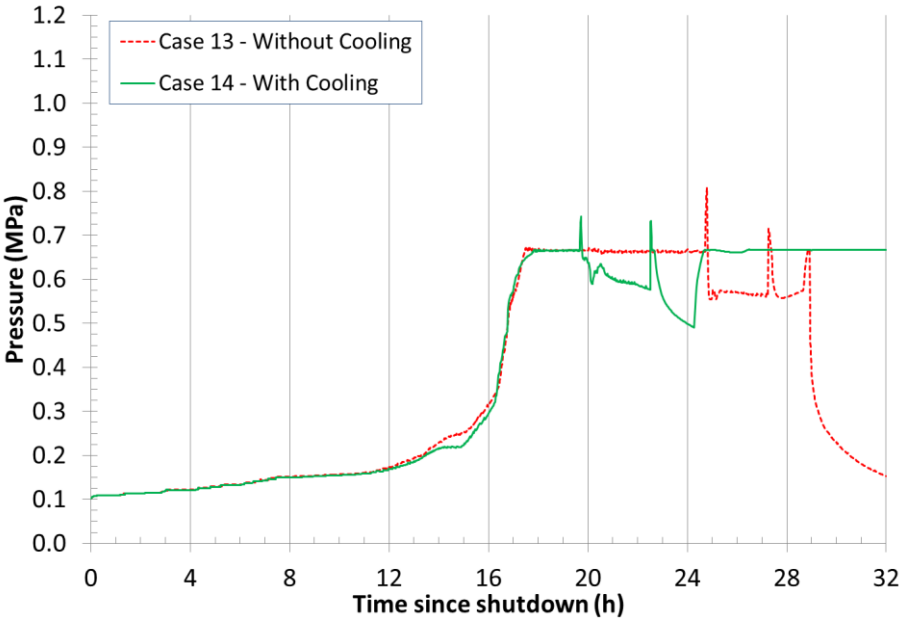

Figure A-7. LTSBO Cases 13 & 14: DW pressure.

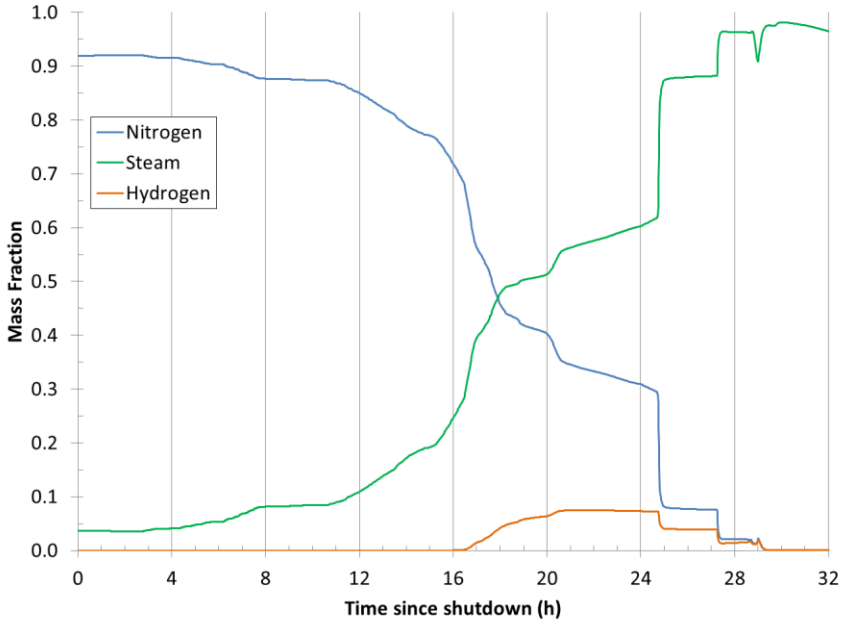

Figure A-8. LTSBO Case 13: DW head region gas concentrations.

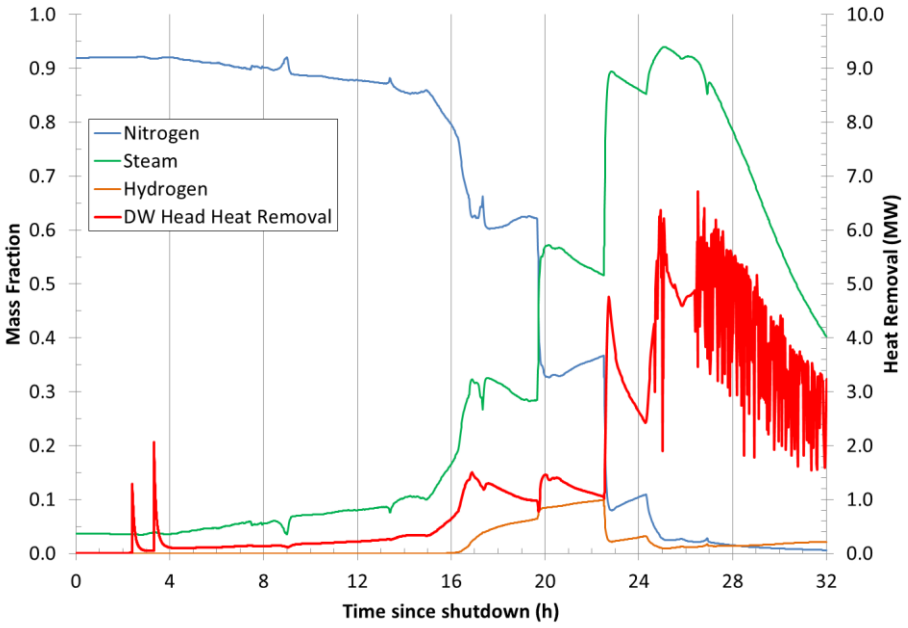

Figure A-9. LTSBO Case 14: DW head region gas concentrations and heat removal.

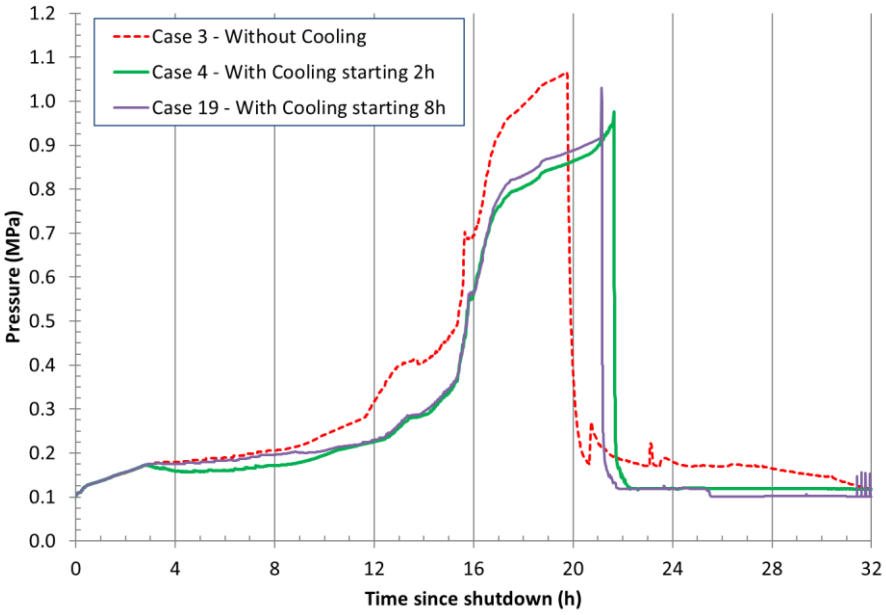

Figure A-10. LTSBO Cases 3, 4 & 19: DW pressure.

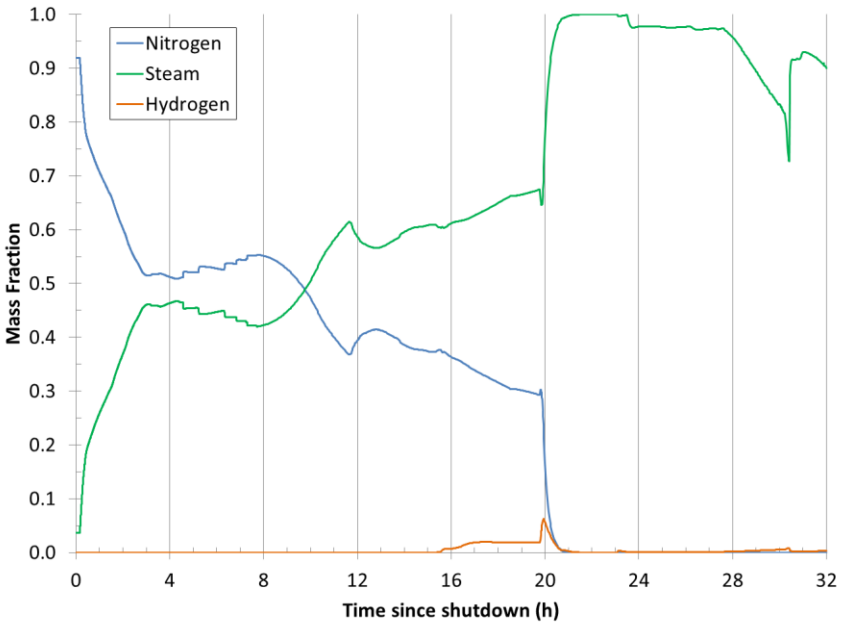

Figure A-11. LTSBO Case 3: DW gas concentrations.

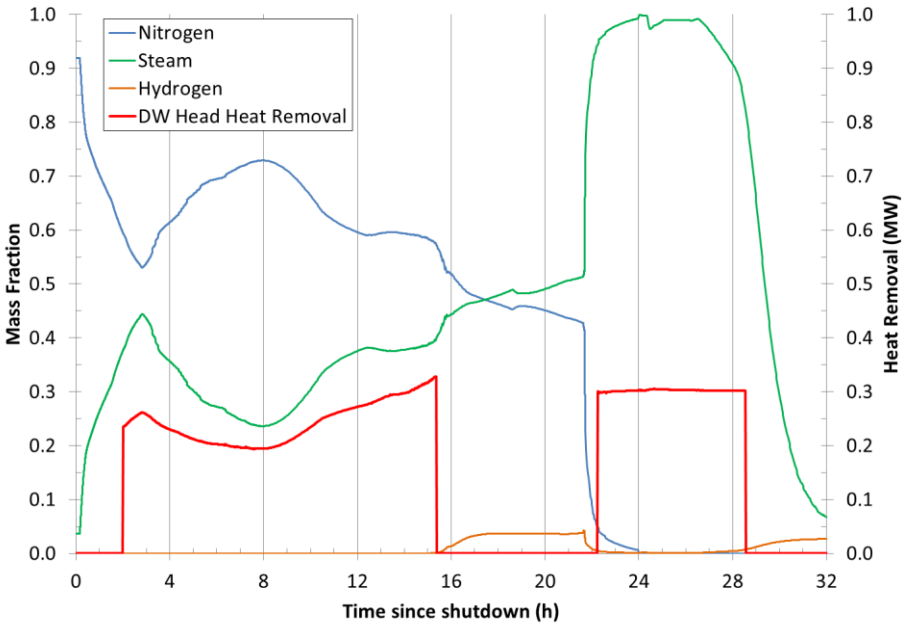

Figure A-12. LTSBO Case 4: DW gas concentrations and heat removal.

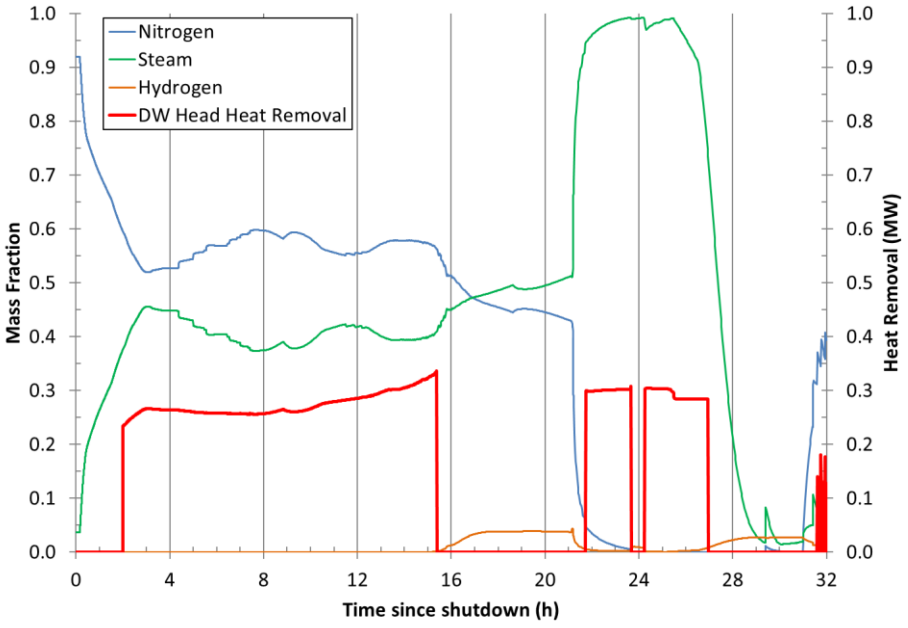

Figure A-13. LTSBO Case 19: DW gas concentrations and heat removal.

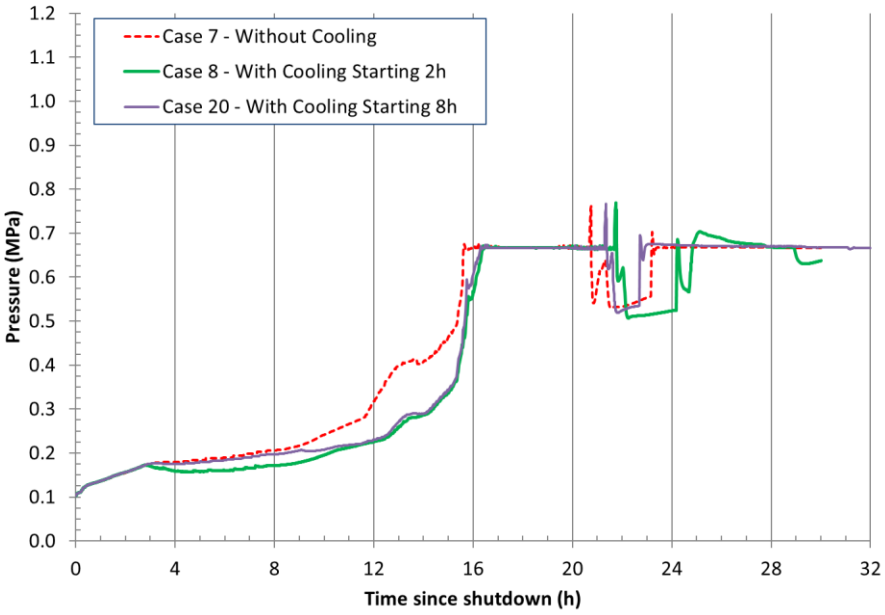

Figure A-14. LTSBO Cases 7, 8 & 20: DW pressure.

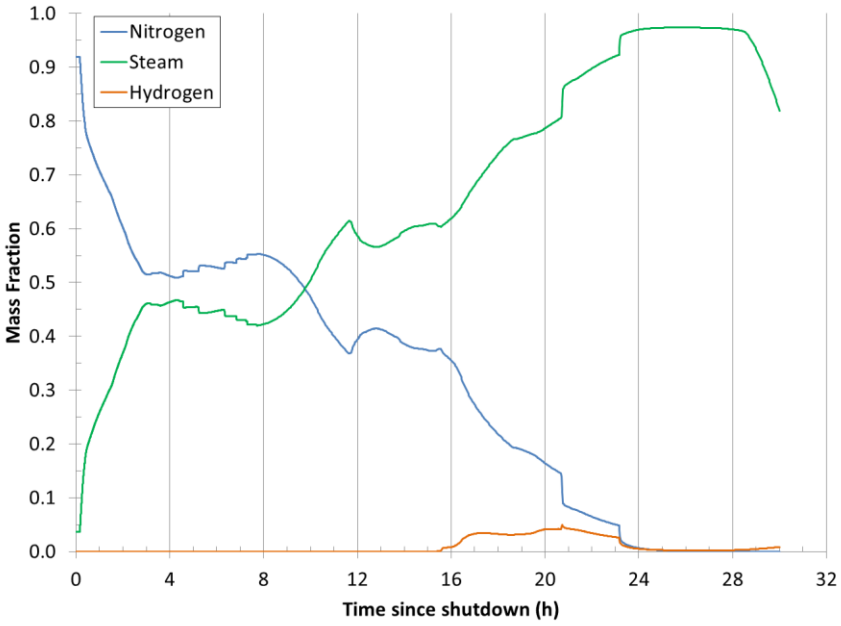

Figure A-15. LTSBO Case 7: DW gas concentrations.

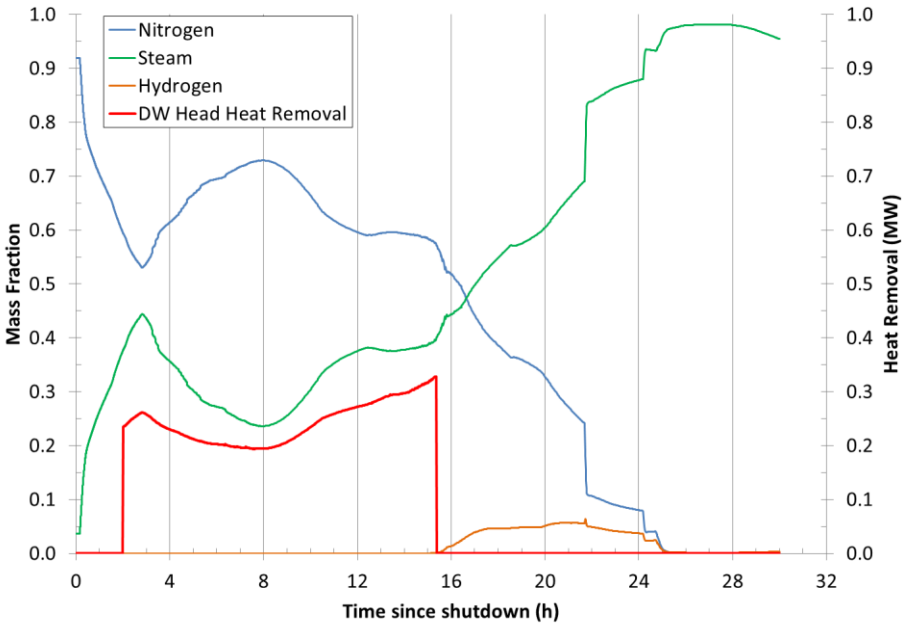

Figure A-16. LTSBO Case 8: DW gas concentrations and heat removal.

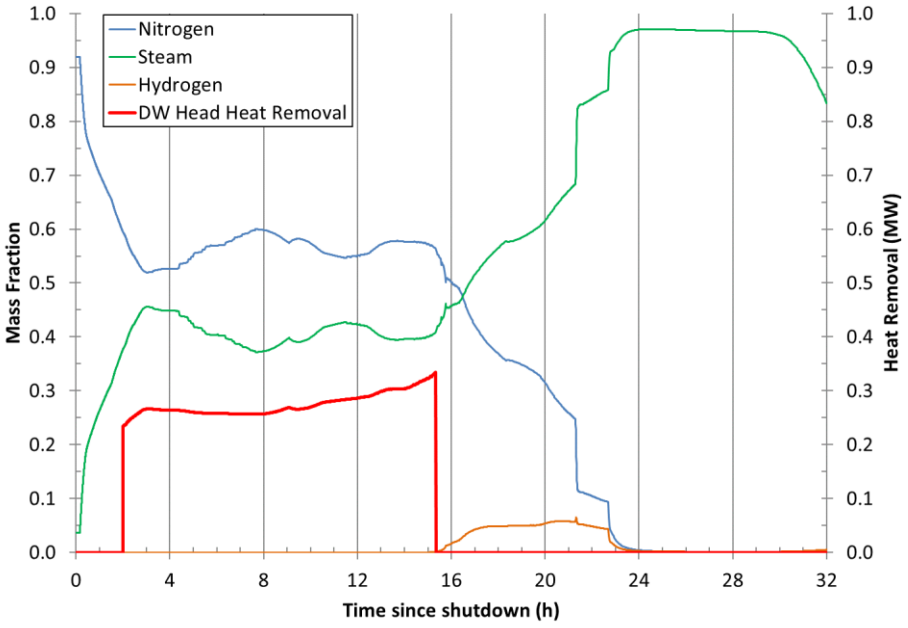

Figure A-17. LTSBO Case 8: DW gas concentrations and heat removal.

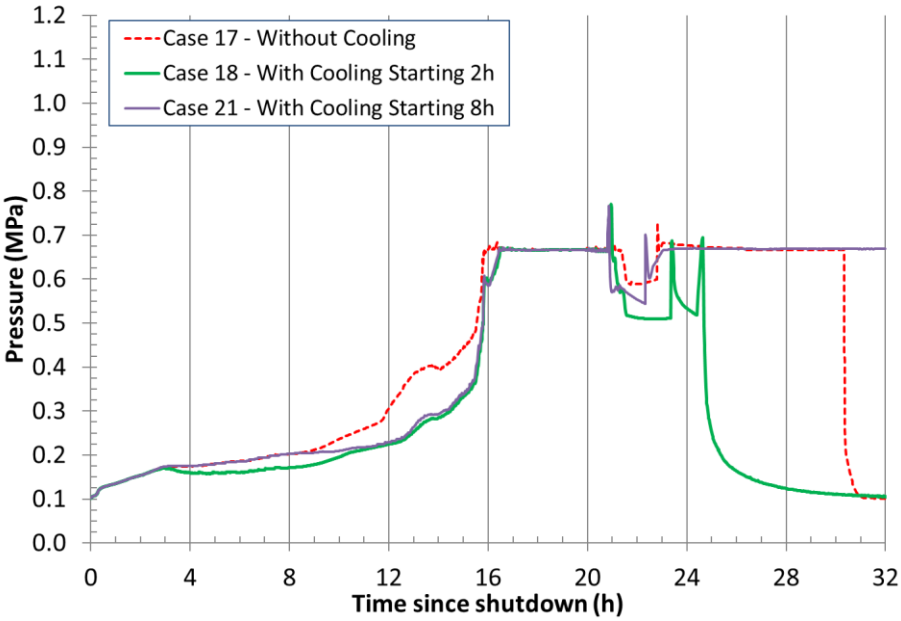

Figure A-18. LTSBO Cases 17, 18 & 21: DW pressure.

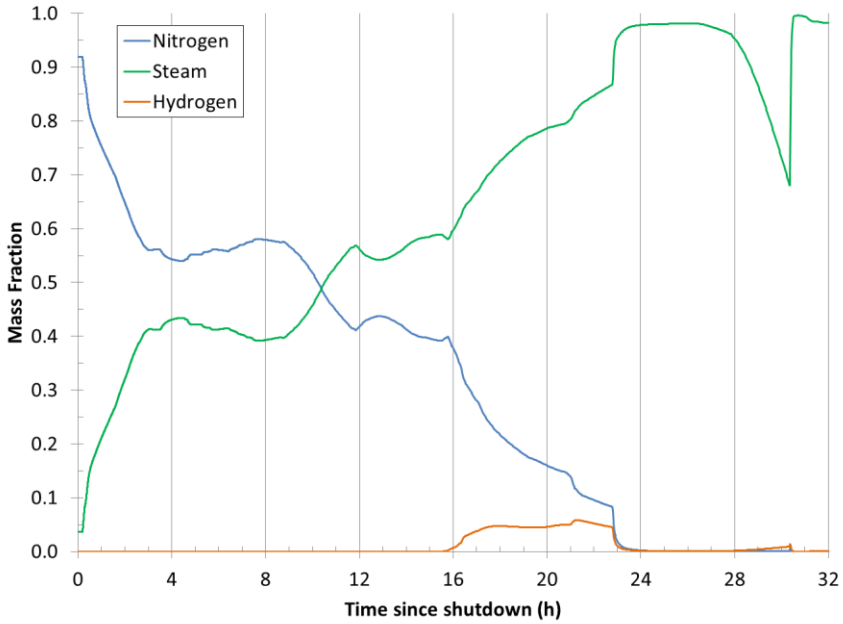

Figure A-19. LTSBO Case 17: DW head region gas concentrations.

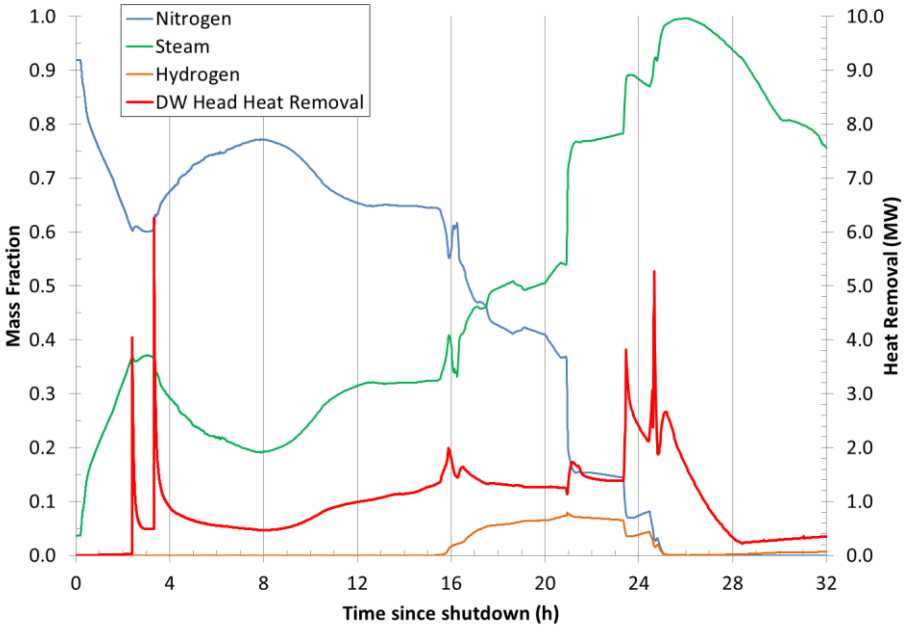

Figure A-20. LTSBO Case 18: DW head region gas concentrations and heat removal.

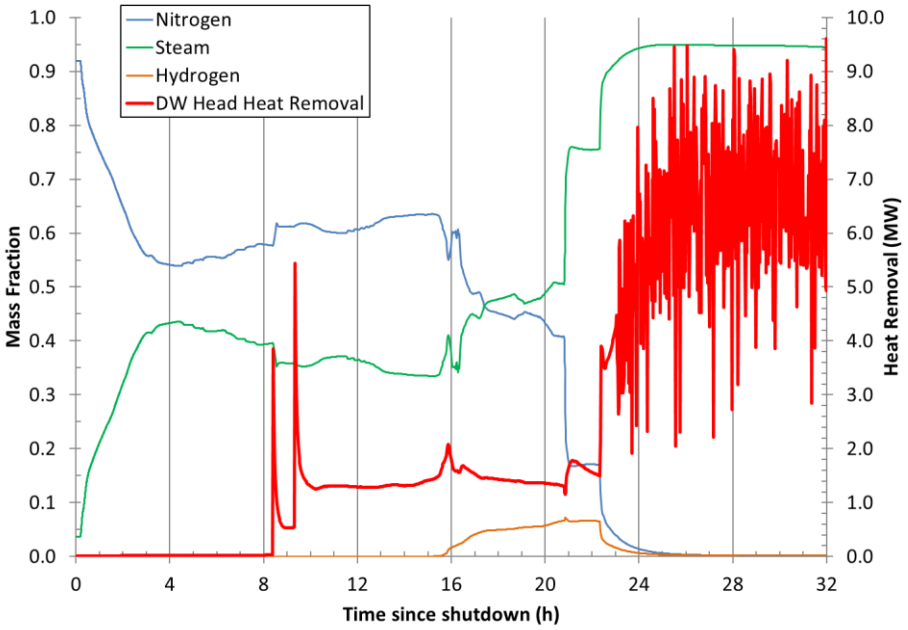

Figure A-21. LTSBO Case 21: DW head region gas concentrations and heat removal.

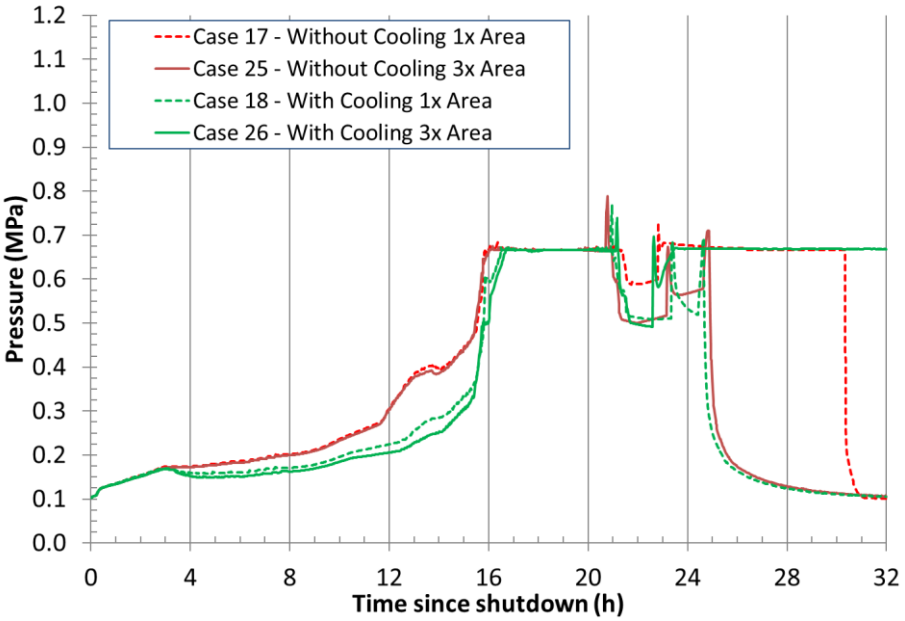

Figure A-22. LTSBO Cases 17, 18, 25 & 26: DW pressure.

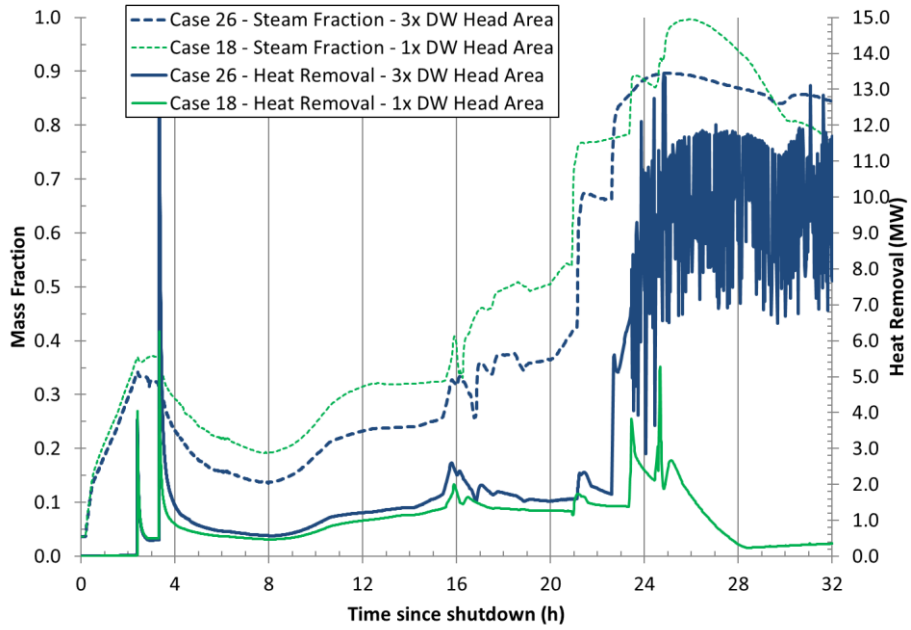

Figure A-23. LTSBO Cases 18 & 26: DW head region steam concentrations and heat removal.

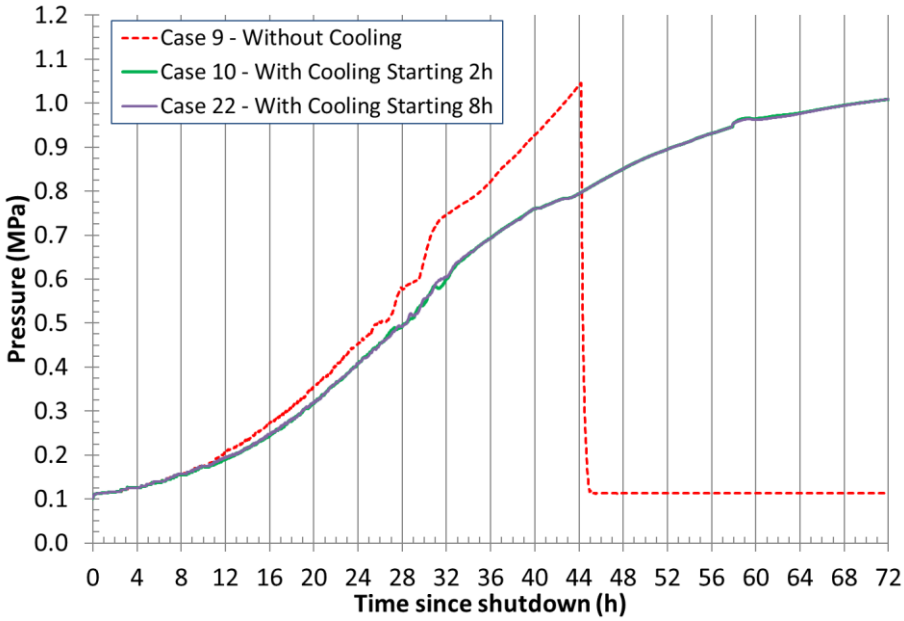

Figure A-24. ELAP Cases 9, 10 & 22: DW pressure.

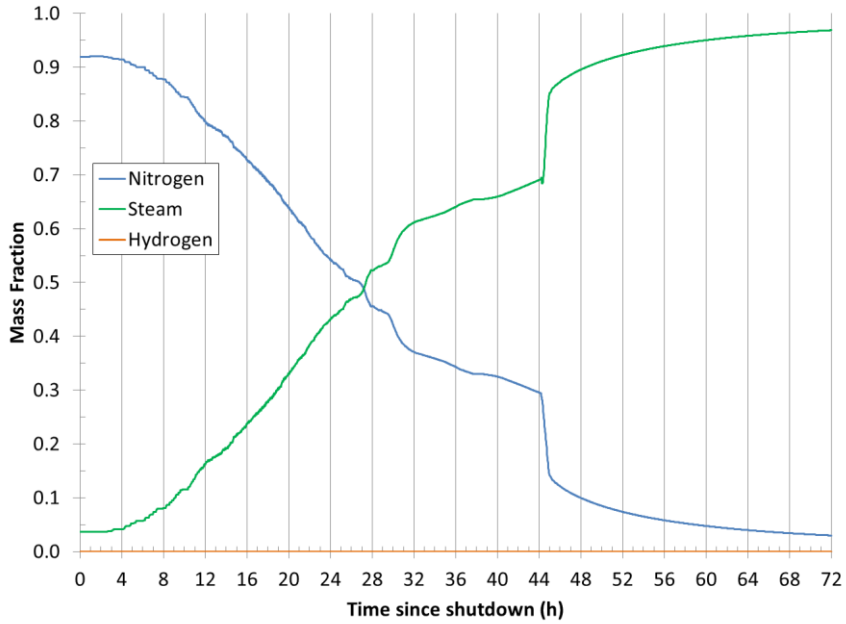

Figure A-25. ELAP Case 9: DW gas concentrations.

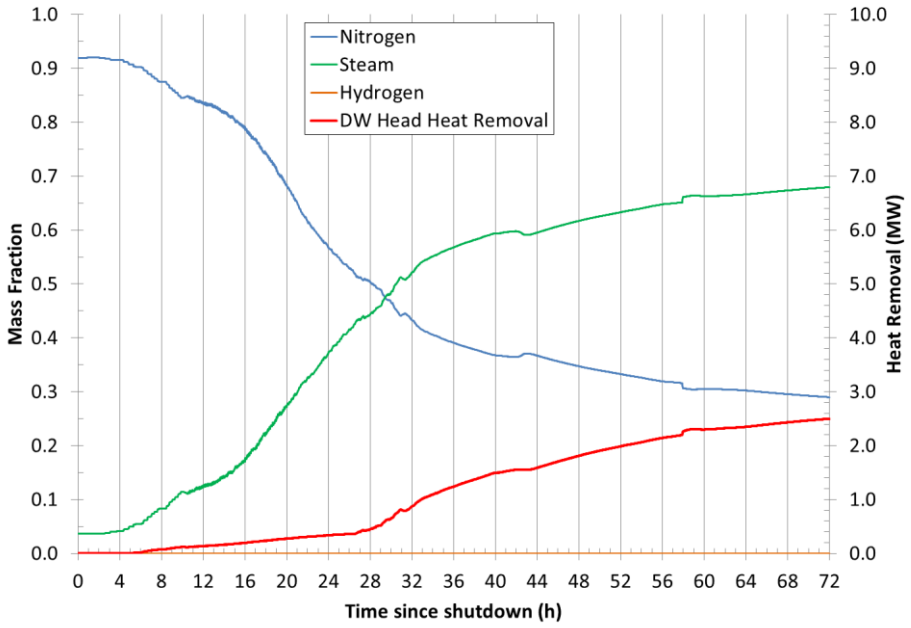

Figure A-26. ELAP Case 10: DW gas concentrations and heat removal.

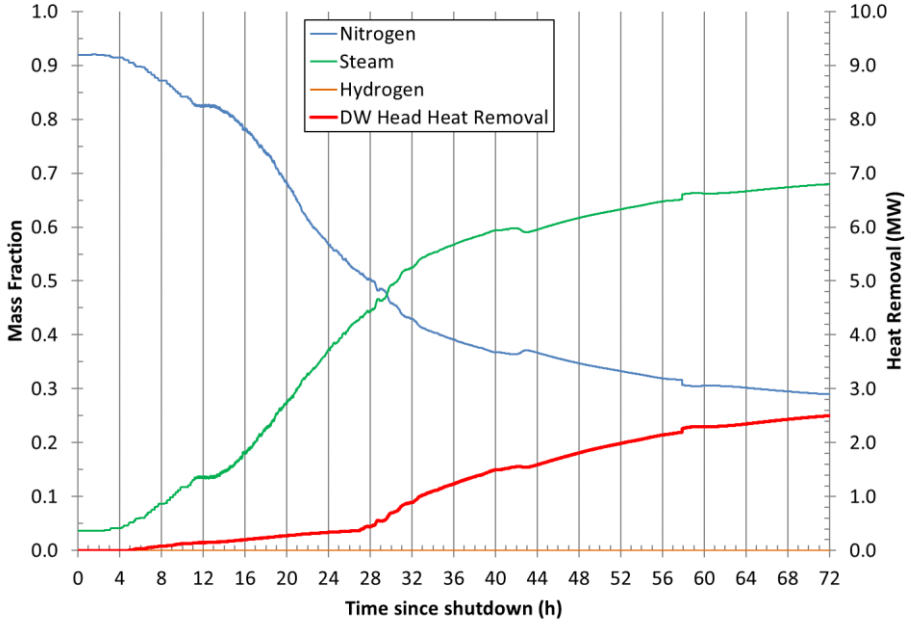

Figure A-27. ELAP Case 22: DW gas concentrations and heat removal.

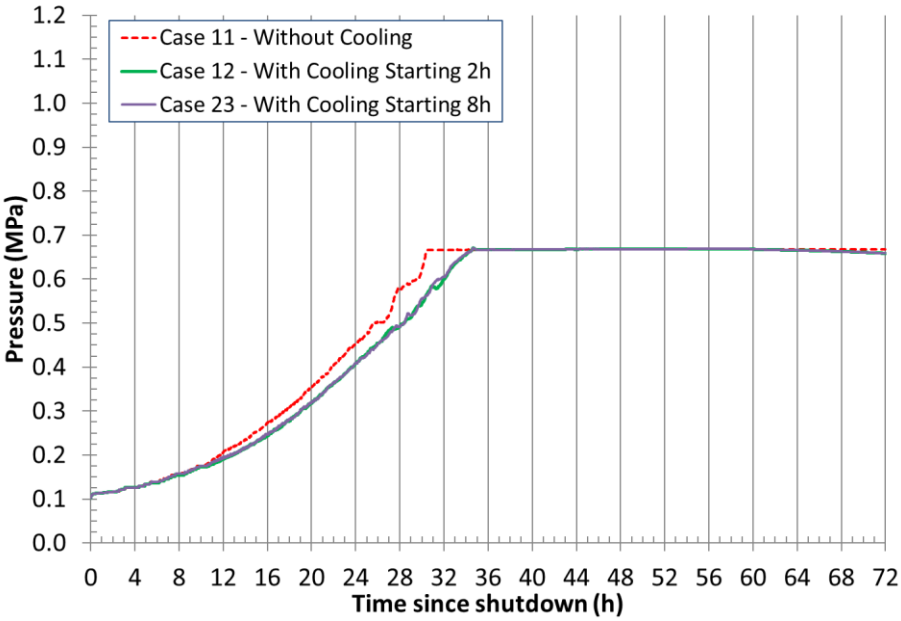

Figure A-28. ELAP Cases 11, 12 & 23: DW pressure.

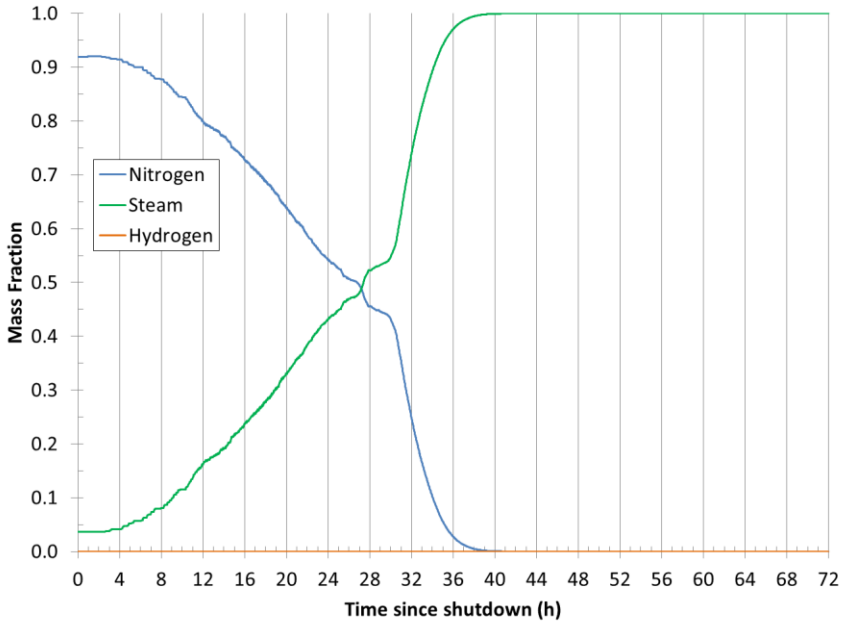

Figure A-29. ELAP Case 11: DW gas concentrations.

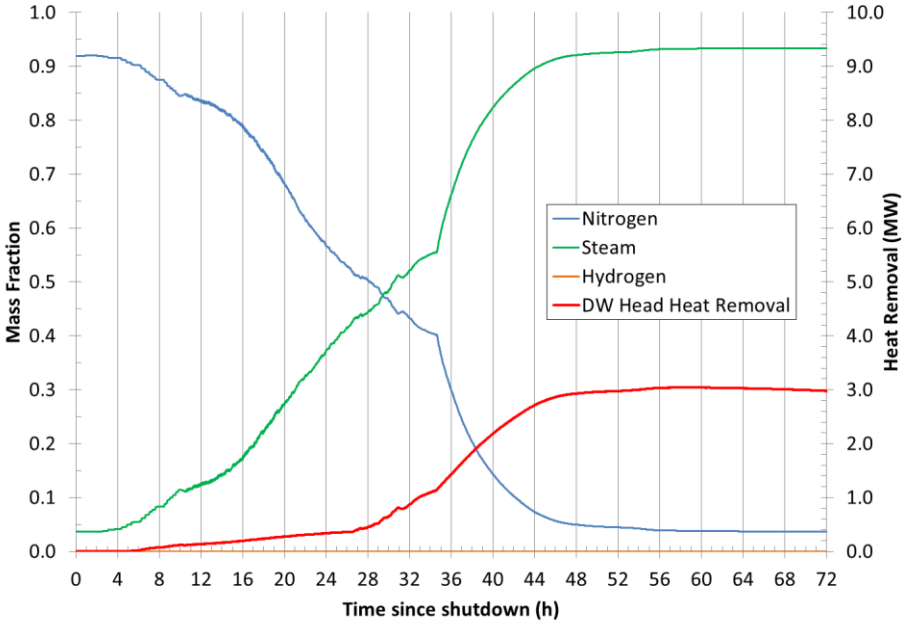

Figure A-30. ELAP Case 12: DW gas concentrations and heat removal.

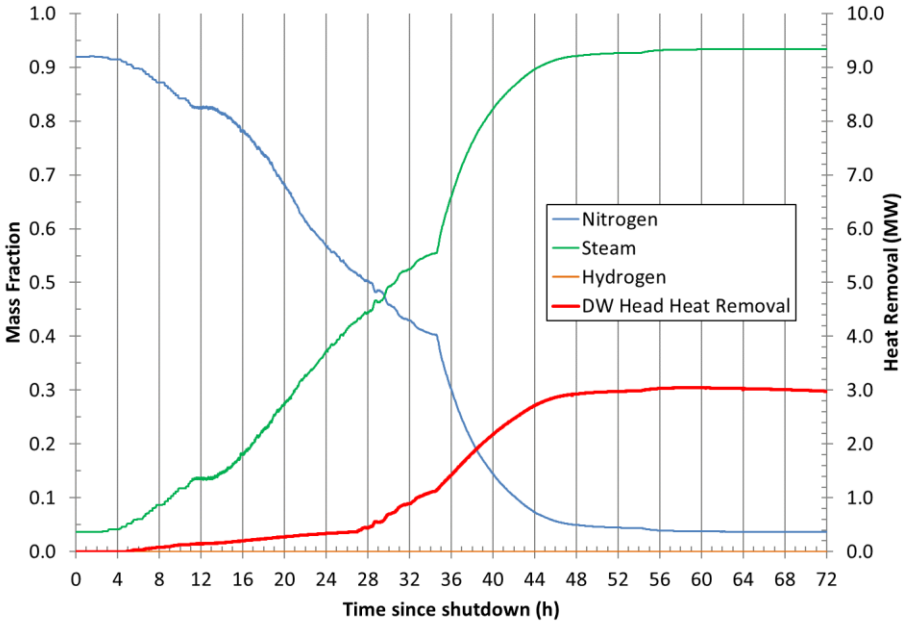

Figure A-31. ELAP Case 23: DW gas concentrations and heat removal.

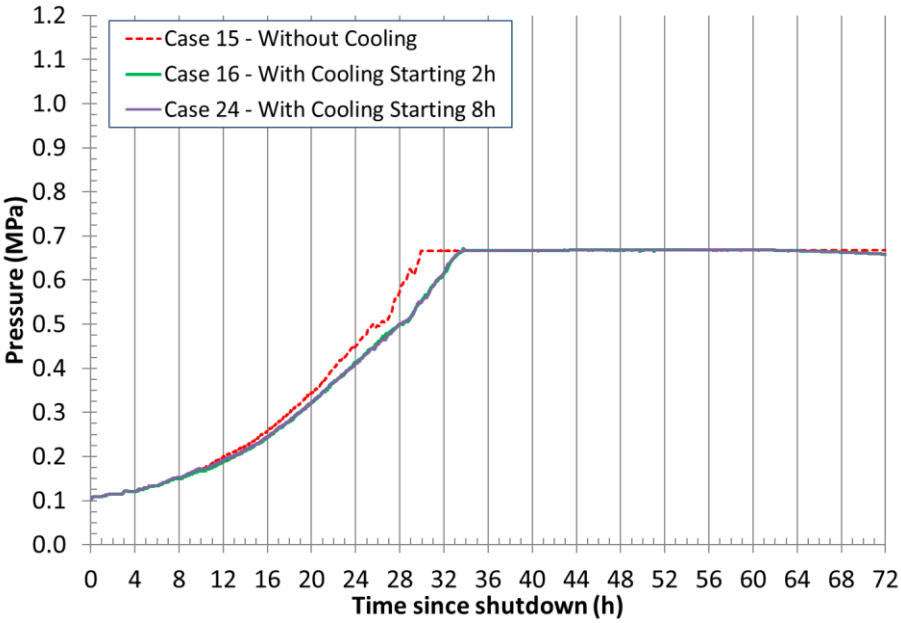

Figure A-32. ELAP Cases 15, 16 & 24: DW pressure.

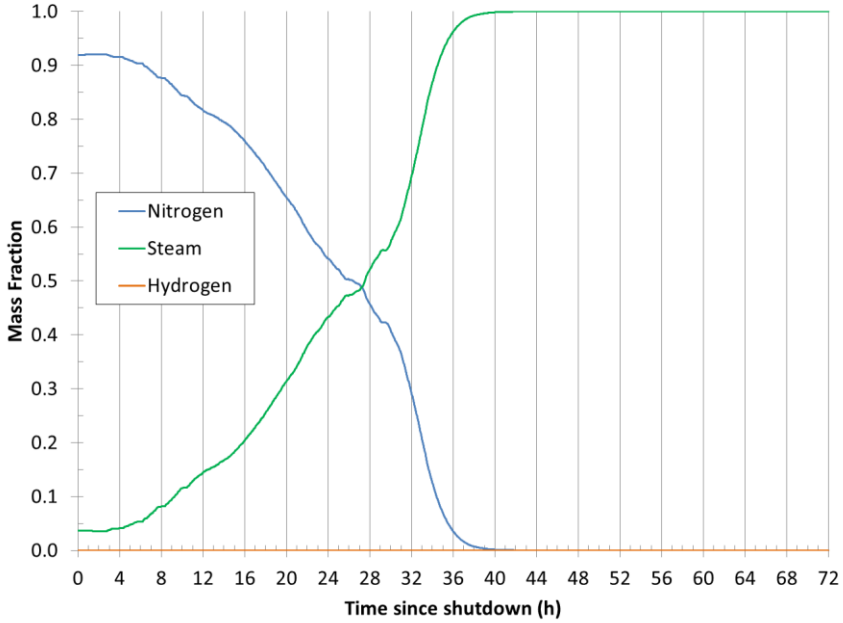

Figure A-33. ELAP Case 15: DW head region gas concentrations.

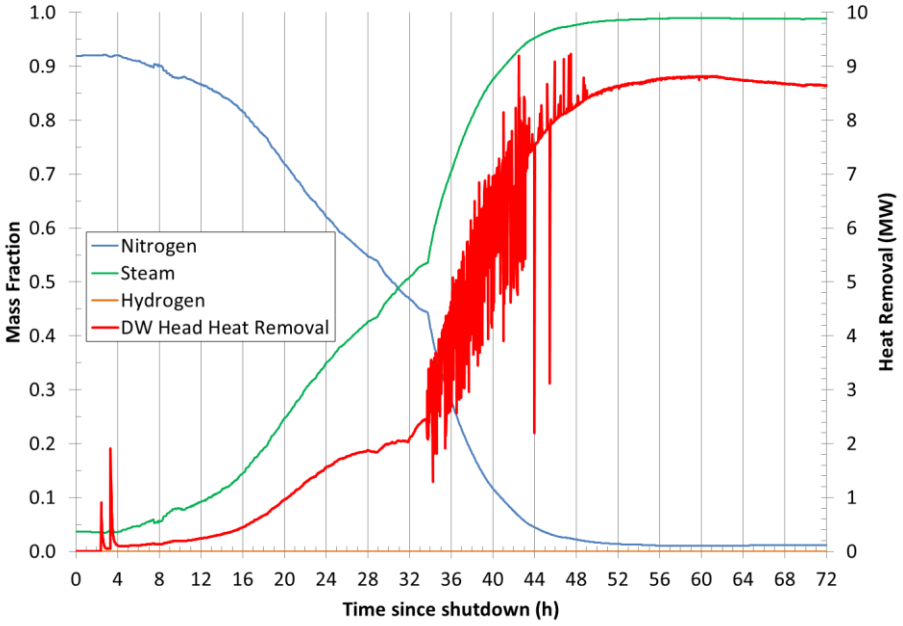

Figure A-34. ELAP Case 16: DW head region gas concentrations and heat removal.

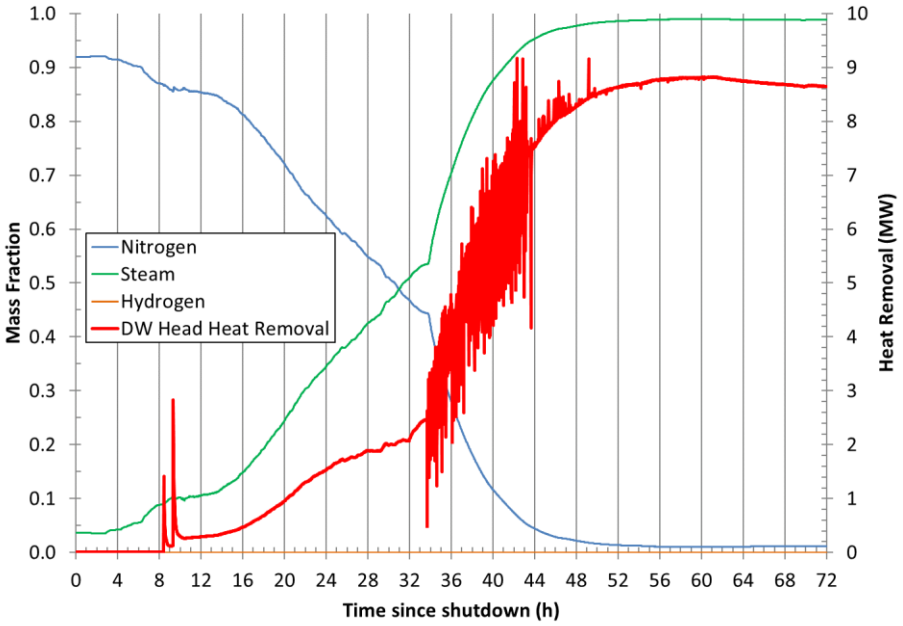

Figure A-35. ELAP Case 24: DW head region gas concentrations and heat removal.

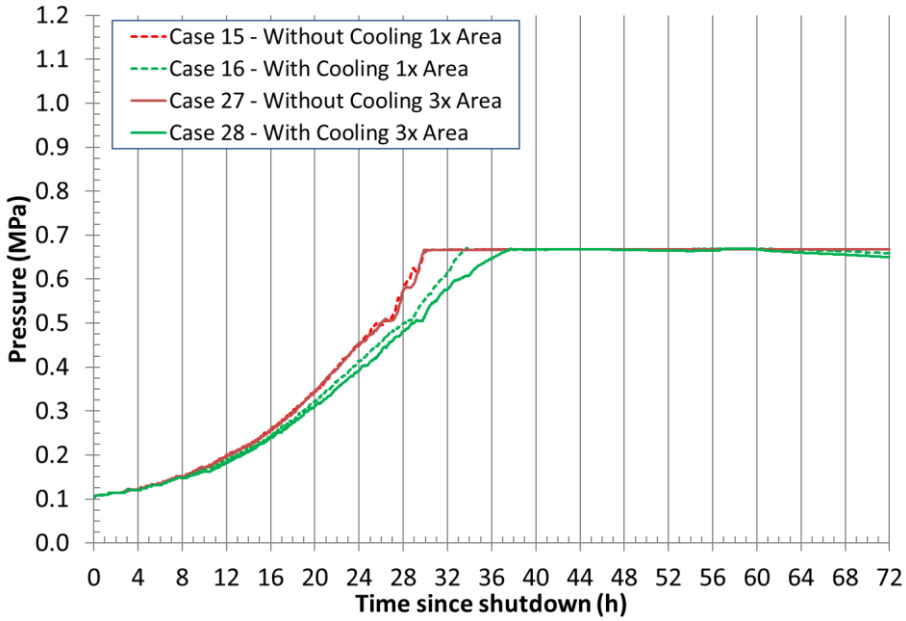

Figure A-36. ELAP Cases 15, 16, 27 & 28: DW pressure.

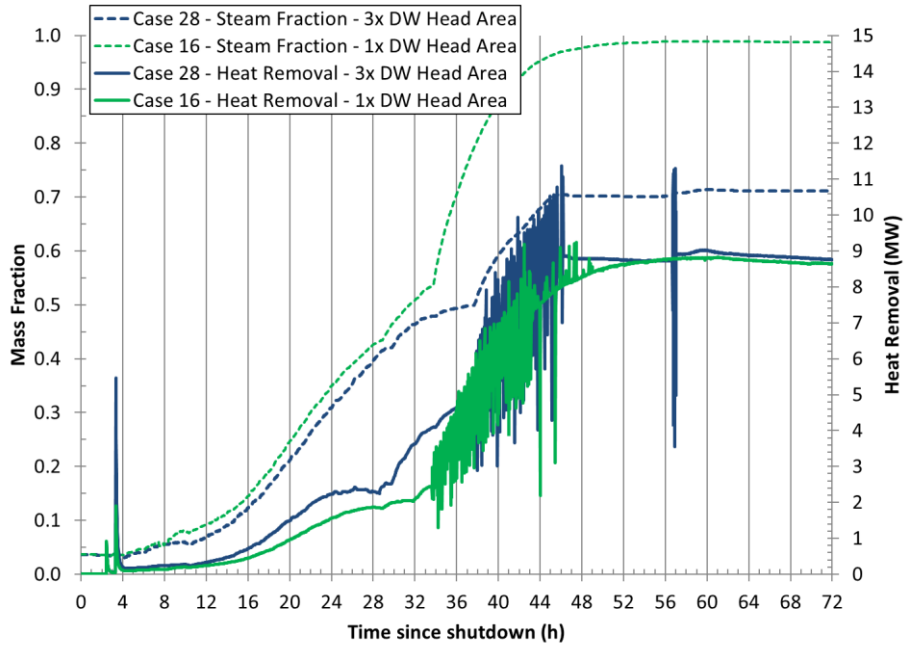

Figure A-37. ELAP Cases 16 & 28: DW head region heat removal.